Electronic Supplementary Material (ESI) for Materials Chemistry Frontiers.

Amphiphilic Rhomboidal Metallacycles with Aggregation-Induced Emission and Aggregation-Caused Quenching Luminogens for White-Light Emission and Bioimaging

Yiqi Fan,[†,#] Jinjin Zhang,[†,#] Yang Li,*[,†] Qi Chen,[‡] Zhigang Ni,[†] Hui Zhou,[†] Jialin Yu,[†] Huayu Qiu,[†] and Shouchun Yin*[,†]

[†]*College of Material, Chemistry and Chemical Engineering, Key Laboratory of Organosilicon Chemistry and Material Technology of Ministry of Education, Hangzhou Normal University, Hangzhou 311121, P. R. China*

[‡]*Institute of Translational Medicine and the Cancer Institute of the Second Affiliated Hospital, Zhejiang University School of Medicine, Hangzhou 310029, P. R. China*

Fax: (+86)57128865077; Tel: (+86)57128865077;

E-mail: yinsc@hznu.edu.cn; liyang@hznu.edu.cn

Contents

1. Materials and methods

All reagents and deuterated solvents were commercially available and used as supplied without further purification. Compounds **4**[S1], **7**[S2], $Pt(PEt_3)_4$[S2] and **8**[S3] were prepared according to the literature procedures. NMR spectra were recorded on a Bruker Advance 500 MHz spectrometer. ^1H and ^{13}C NMR chemical shifts are reported relative to residual solvent signals, and $^{31}P\{^1H\}$ NMR chemical shifts are referenced to an external unlocked sample of 85.0 % H_3PO_4 (δ = 0.0 ppm). Mass spectra were recorded on a Micro mass Quattro II triple-quadrupole mass spectrometer with a MassLynx operating system and 6530 Q-TOF LC/MS. The melting points were collected on a YRT-3 automatic melting point apparatus. The UV-vis absorption spectra were measured by a Hitachi U-5300 absorption spectrophotometer. The fluorescent emission spectra were conducted on a Hitachi F-7000 fluorescence spectrophotometer and quantum yields were determined using quinine sulfate as reference at a concentration of 10.0 μM and the excited wavelength of 365 nm. Transmission Electron Microscopy (TEM) was performed on a Hitachi S-4800. Dynamic light scattering (DLS) experiments were performed using a Nano ZS90 instrument with a He-Ne laser (633 nm) and 90° collecting optics. The data were analyzed using the Malvern Dispersion Technology Software 5.10. 3-(4,5-Dimethylthiazol-2-yl)-2,5-diphenyltetrazolium bromide (MTT), trypsine-EDTA, fetal bovine serum (FBS) and DiO fluorescence probe were purchased from Sigma-Aldrich. Dulbecco's modified eagle medium (DMEM) and Penicillin-Streptomycin were purchased from Birstol-Myers Squibb Trading Co. Ltd. Fluorescence imaging of cells was observed by confocal laser scanning microscopy (CLSM, Radiance 2100, Bio-Rad). Fluorescence intensity of cells was measured by a FACS Calibur flow cytometer (BD Biosciences, USA).

2. Synthetic procedures and characterization data

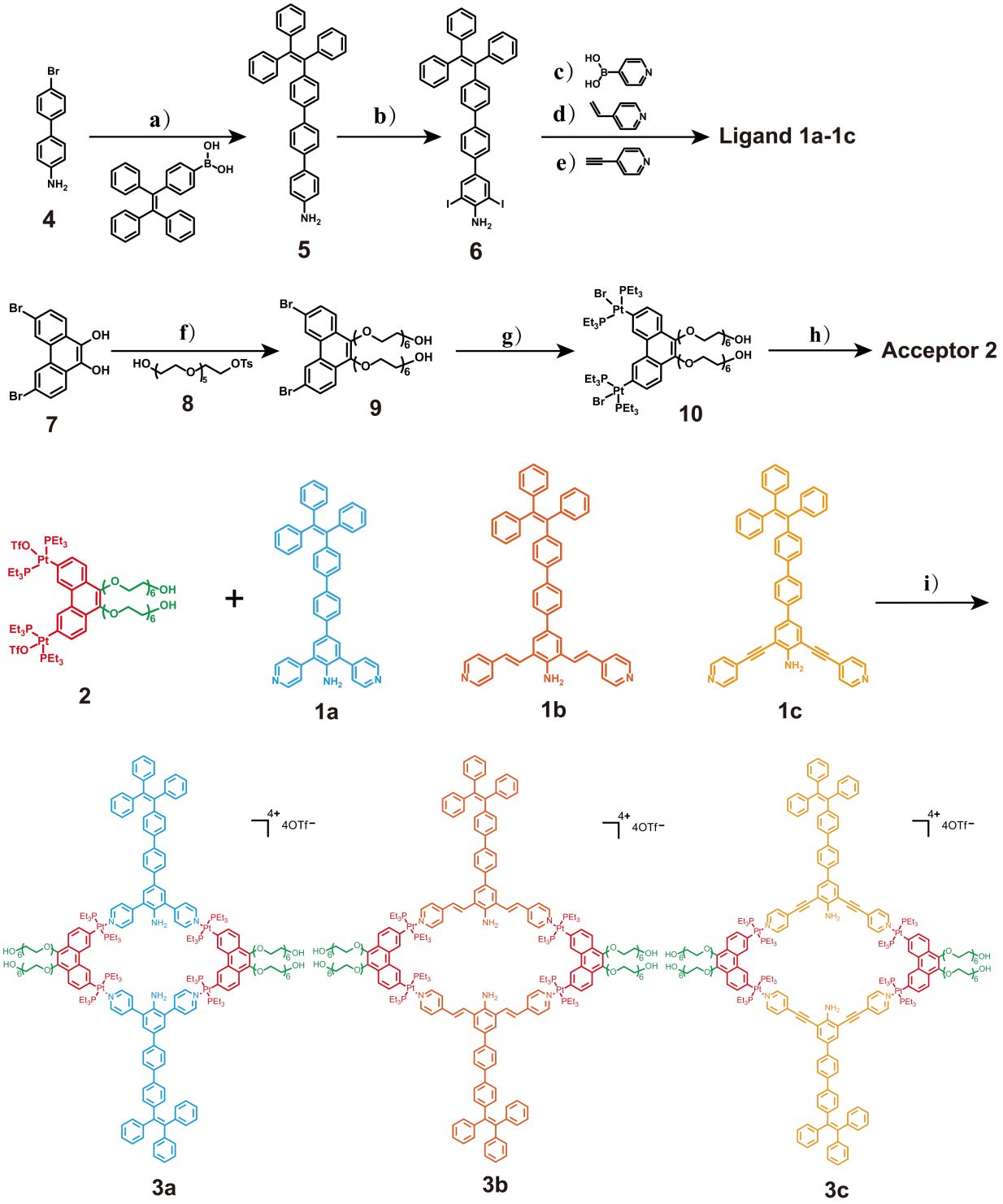

Scheme S1 Synthetic routes to ligands **1a-1c**, acceptor **2** and metallacycle **3a-3c** and chemical structures of compounds used in this study. Conditions: (a) K_2CO_3, $Pd(PPh_3)_4$, 1,4-dioxane/water (4:1 *v*/*v*), 85 °C, 48 h, 43.4%; (b) ICl, CH_2Cl_2, 40 °C, 24 h, 20.8%; (c) K_2CO_3, $Pd(PPh_3)_4$, 1,4-dioxane/water (4:1 *v*/*v*), 85 °C, 48 h, 30.9%; (d) Et_3N, CuI, $Pd(PPh_3)_4$, THF, 60 °C, 48 h, 20.0%; (e) Et_3N, PPh_3, $Pd(OAc)_2$, DMF, 90 °C, 48 h, 23.0%; (f) K_2CO_3, DMF, 90 °C, 24 h, 57.6%; (g) $Pt(PEt_3)_4$, toluene, 95 °C, 72 h, 91.1%; (h) AgOTf, CH_2Cl_2, room temperature, 12 h, 92.3%; (i) CH_3OH, 55 °C, 12 h, 84.3%.

*2.1 Synthesis of compound **4***

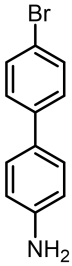

Compound **4** was synthesized according to literature procedure[S1]. The ^{1}H NMR of **4** matches well with the reported data. ^{1}H NMR (500 MHz, $CDCl_3$, 298K) δ (ppm): 7.51 (d, J = 8.5 Hz, 2H), 7.42–7.34 (m, 4H), 6.75 (d, J = 8.5 Hz, 2H), 3.75 (s, 2H).

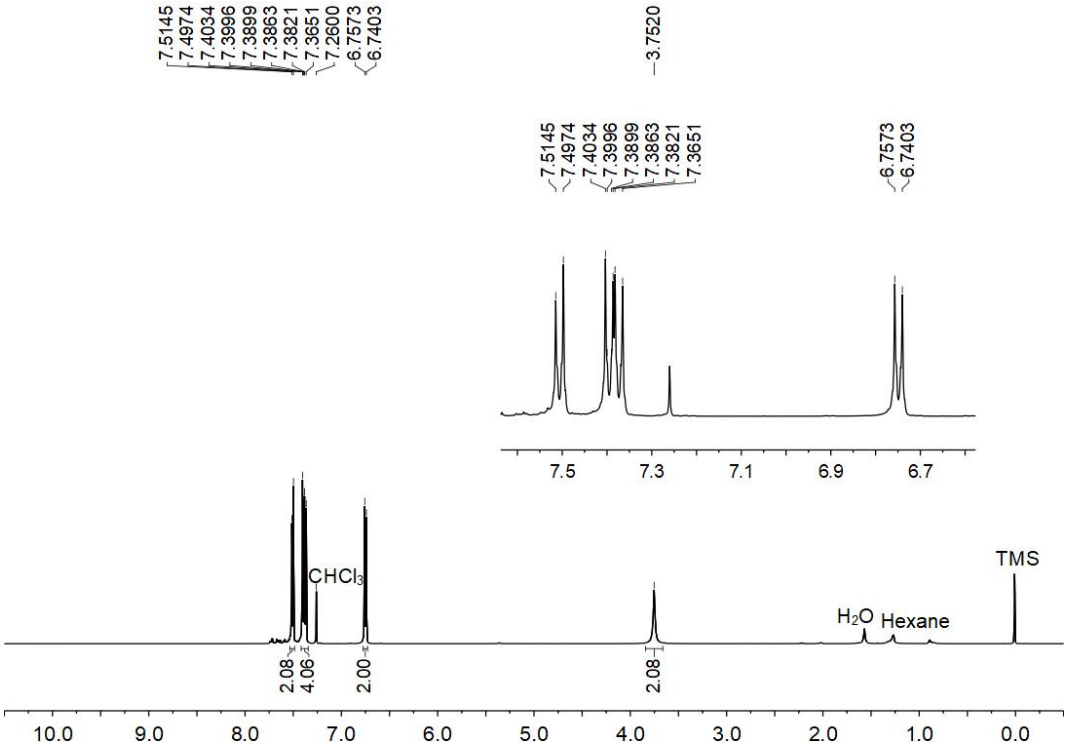

Figure S1. ^{1}H NMR spectrum (500 MHz, $CDCl_3$, 298 K) recorded for **4**.

*2.2 Synthesis of compound **5***

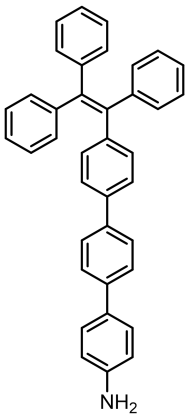

Compound **4** (0.5 g, 2.02 mmol), (4-(1,2,2-triphenylvinyl)phenyl)boronic acid (1.1 g, 3.03 mmol), K_2CO_3 (1.4 g, 10.10 mmol), $Pd(PPh_3)_4$ (26.4 mg, 0.02 mmol) were added to 250 mL Schlenk flask and then dissolved in 1,4-dioxane/H_2O (150 mL, 4/1, *v*/*v*) under nitrogen. The mixture was stirred at 85 ℃ for 48 h. After cooling to room temperature, the mixture was filtered and the solvent was removed in vacuo. Then the mixture was extracted with CH_2Cl_2/H_2O three times, dried over anhydrous $MgSO_4$, filtered and removed to give a crude product. The crude product was further purified by flash column chromatography with petroleum ether/ethyl acetate (6:1, *v*/*v*) as the eluent to afford compound **5** as a yellow solid (705.0 mg, 43.4%). M. P. 248–250 ℃. ^{1}H NMR (500 MHz, CD_3SOCD_3, 298 K) δ (ppm): 7.62 (d, J = 8.6 Hz, 2H), 7.59 (d, J = 8.6 Hz, 2H), 7.49 (d, J = 8.3 Hz, 2H), 7.41 (d, J = 8.5 Hz, 2H), 7.19–7.10 (m, 9H), 7.04 (t, J = 8.2 Hz, 6H), 7.01–6.97 (m, 2H), 6.66 (d, J = 8.5 Hz, 2H), 5.27 (s, 2H). ^{13}C NMR (125 MHz, CD_3SOCD_3, 298K) δ (ppm): 149.0, 143.7, 143.7, 142.5, 141.2, 140.6, 140.1, 138.1, 136.7, 131.8, 131.2, 131.2, 128.4, 128.3, 128.3, 127.5, 127.1, 127.1, 127.0, 126.1, 126.0, 114.7.

ESI-HRMS [**5** + H]$^+$: calcd. for $[C_{38}H_{30}N]^+$ 500.2373, found 500.2391.

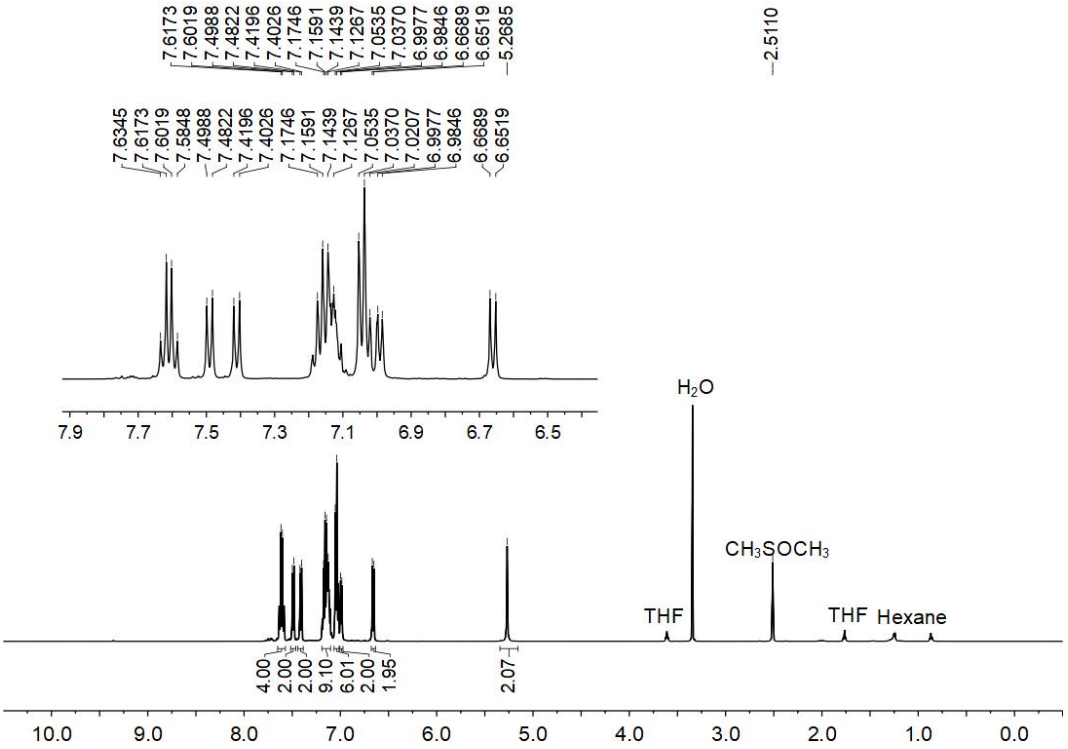

Figure S2. ^{1}H NMR spectrum (500 MHz, CD_3SOCD_3, 298 K) of compound **5**.

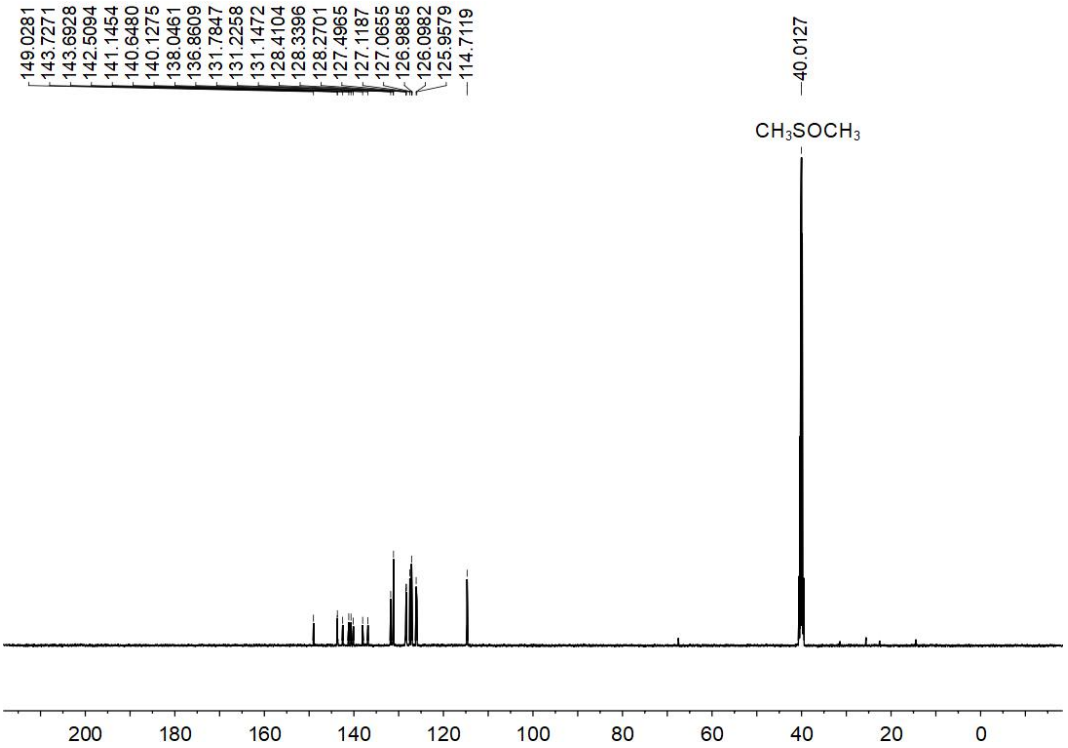

Figure S3. ^{13}C NMR spectrum (125 MHz, CD_3SOCD_3, 298 K) of compound **5**.

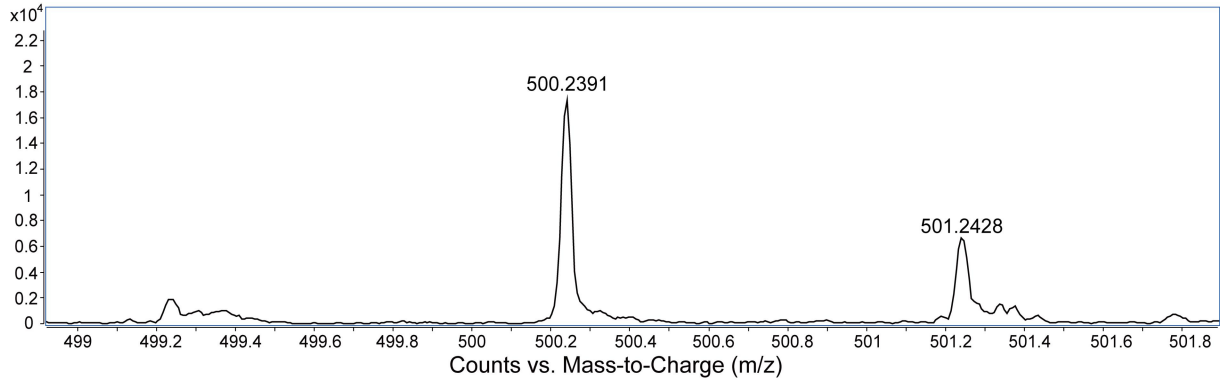

Figure S4. ESI-HRMS spectrum of compound **5**.

2.3 Synthesis of compound ***6***

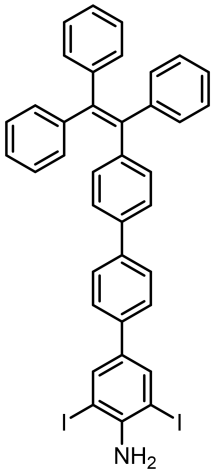

The ICl solution (1.0 mol/L in CH_2Cl_2) was added dropwise into dry CH_2Cl_2 (100 mL) containing compound **5** (500.0 mg, 1.00 mmol), and then the mixture solution was refluxed for 6 h. After cooling to room temperature, the mixture was extracted with CH_2Cl_2/saturated aqueous solution of $Na_2S_2O_3$ three times, dried over anhydrous $MgSO_4$, filtered and removed to give a crude product. The crude product was further purified by flash column chromatography with petroleum ether/ethyl acetate (20:1, *v*/*v*) as the eluent to afford compound **6** as a white solid (100.0 mg, 20.8%). M. P. 181–183 ℃. ^{1}H NMR (500 MHz, CD_3SOCD_3, 298 K) δ (ppm): 7.98 (s, 2H), 7.65–7.49 (m, 6H), 7.23–6.93 (m, 17H), 5.23 (s, 2H). ^{13}C NMR (125 MHz, CD_3SOCD_3, 298K) δ (ppm): 147.1, 143.6, 142.8, 141.2, 140.6, 138.2, 137.7, 137.3, 136.7, 132.2, 131.8, 131.2, 131.1, 128.4, 128.4, 128.3, 127.3, 127.2, 127.1, 126.7, 126.1, 82.8. ESI-HRMS [**6** + K]$^+$: calcd. for $[C_{38}H_{28}I_2NK]^+$ 789.9864, found 789.4427.

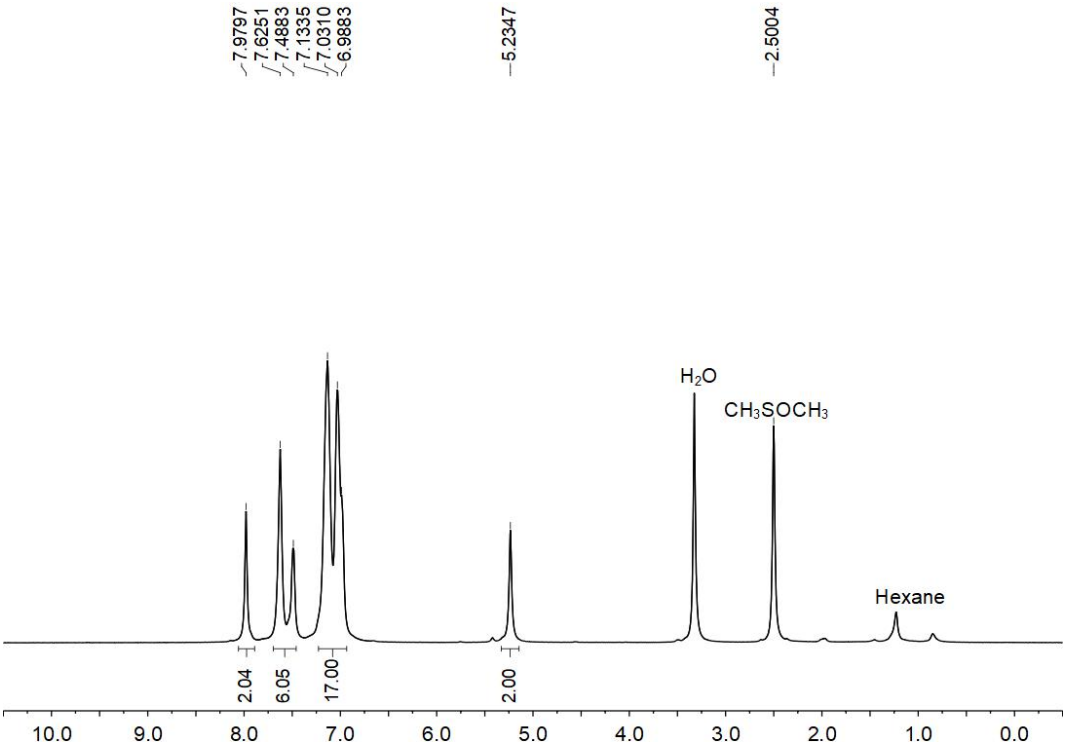

Figure S5. ^{1}H NMR spectrum (500 MHz, CD_3SOCD_3, 298 K) of compound **6**.

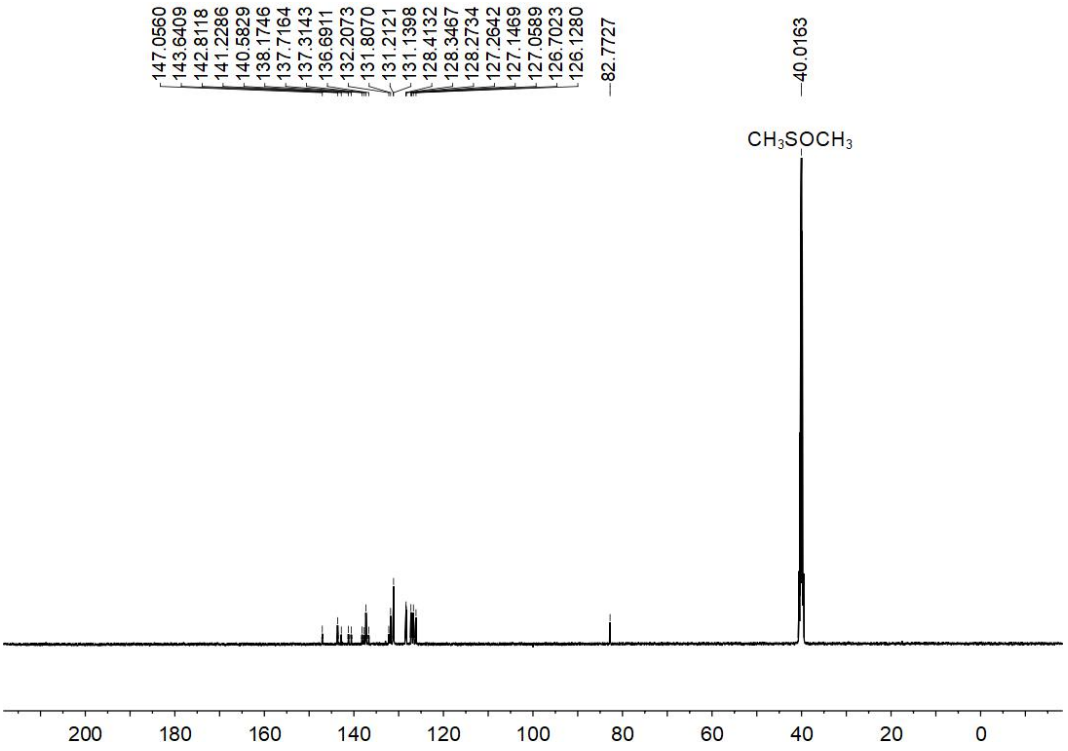

Figure S6. ^{13}C NMR spectrum (125 MHz, CD_3SOCD_3, 298 K) of compound **6**.

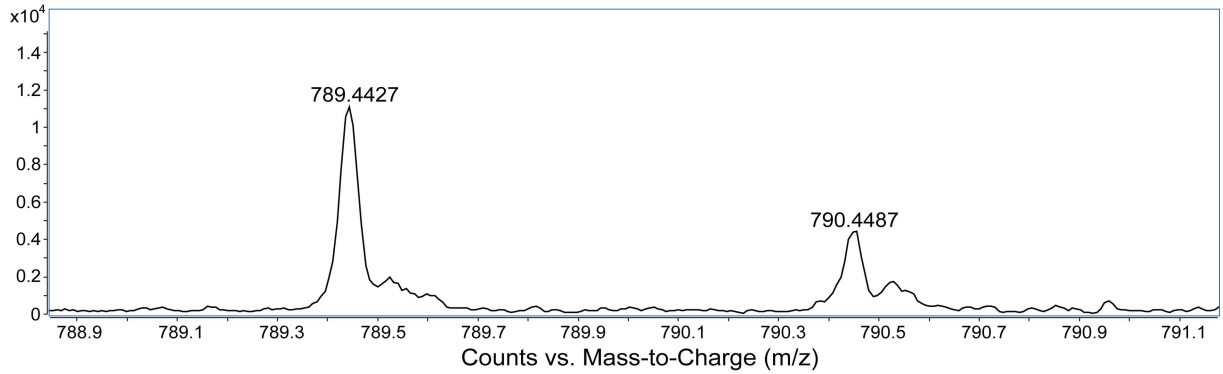

Figure S7. ESI-HRMS spectrum of compound **6**.

*2.4 Synthesis of ligand **1a***

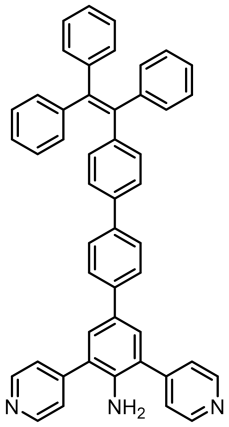

Compound **6** (100.0 mg, 0.13 mmol), 4-pyridineboronic acid (81.9 mg, 0.67 mmol), K_2CO_3 (183.0 mg, 1.33 mmol), $Pd(PPh_3)_4$ (15.3 mg, 0.01 mmol) were dissolved in 1,4-dioxane/H_2O (50 mL, 4/1, *v*/*v*) under nitrogen, and then the mixture solution was stirred at 85 °C for 48 h. After cooling to room temperature, the mixture was filtered and the solvent was removed in vacuo. Then the mixture was extracted with CH_2Cl_2/H_2O three times, dried over anhydrous $MgSO_4$, filtered and removed to give a crude product. The crude product was further purified by flash column chromatography with CH_2Cl_2/CH_3OH (30:1, *v*/*v*) as the eluent to afford ligand **1a** as a white solid (30.0 mg, 30.9%). M. P. 174–176 °C. ^{1}H NMR (500 MHz, $CDCl_3$, 298 K) δ (ppm): 8.75 (d, 4H), 7.61 (d, J = 8.6 Hz, 4H), 7.54–7.48 (m, 4H), 7.45 (s, 2H), 7.38 (d, J = 8.3 Hz, 2H), 7.15–7.03 (m, 17H), 3.95 (s, 2H). ^{13}C NMR (125 MHz, $CDCl_3$, 298K) δ (ppm): 150.7, 147.3, 143.8, 143.7, 143.7, 142.9, 141.2, 140.5, 139.7, 139.2, 138.6, 138.20, 131.9, 131.4, 131.4, 128.9, 127.8, 127.7, 127.7, 127.3, 126.6, 126.5, 126.0, 125.8. ESI-HRMS [**1a** + K]$^+$: calcd. for $[C_{48}H_{36}N_3K]^+$ 654.2904, found 654.2981.

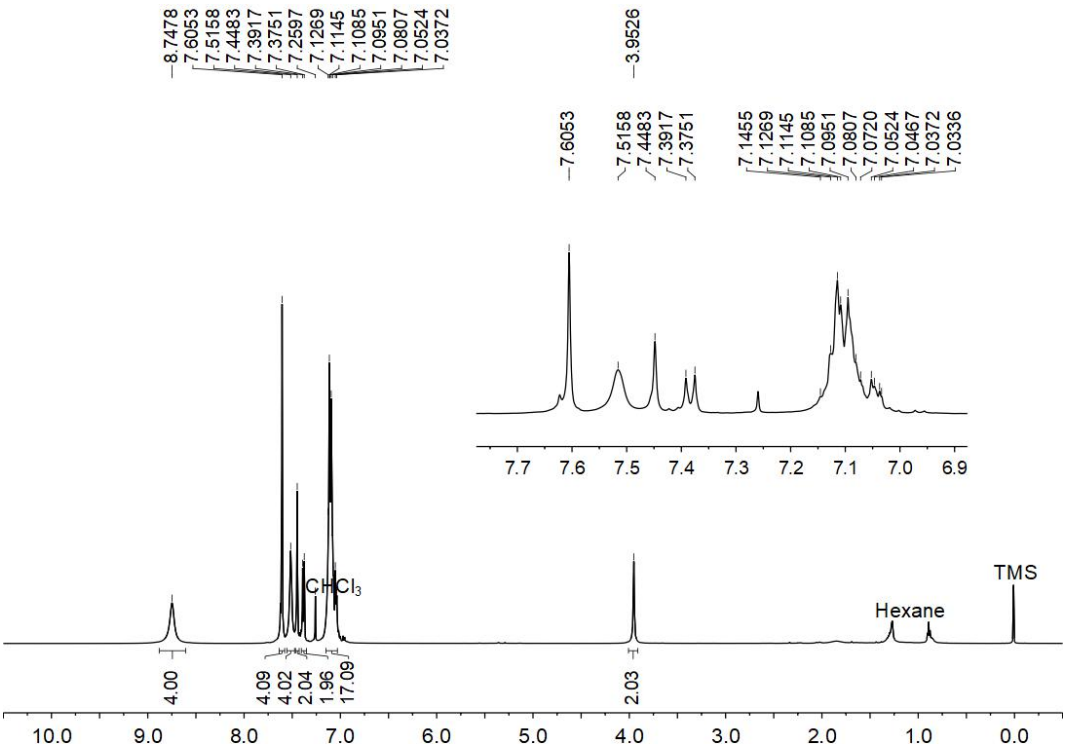

Figure S8. ^{1}H NMR spectrum (500 MHz, $CDCl_3$, 298K) of ligand **1a**.

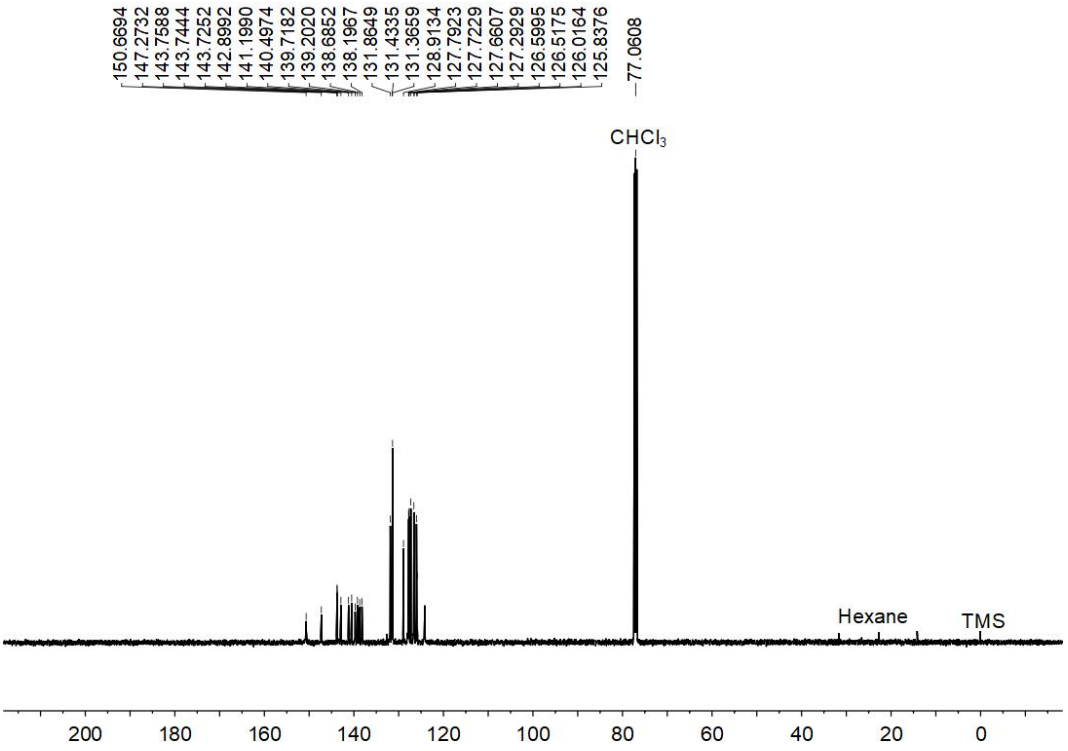

Figure S9. ^{13}C NMR spectrum (125 MHz, $CDCl_3$, 298K) of ligand **1a**.

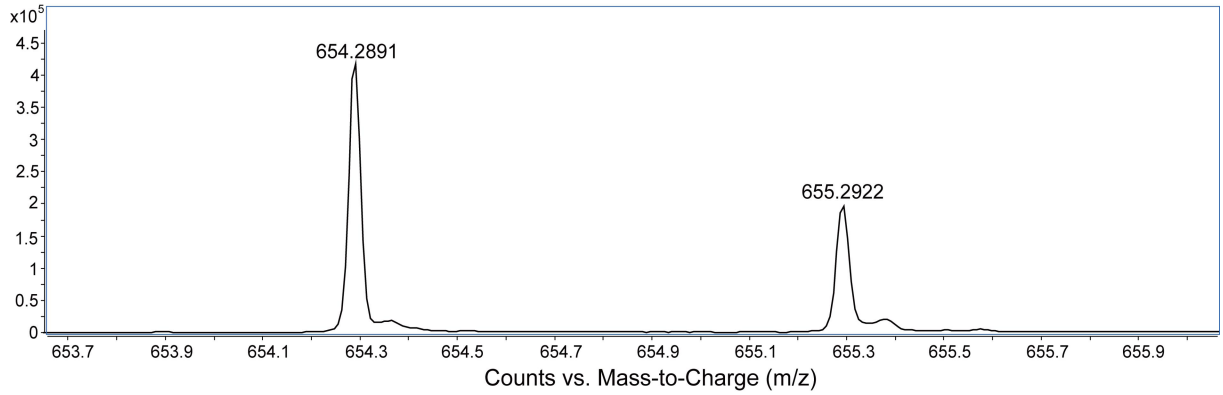

Figure S10. ESI-HRMS spectrum of ligand **1a**.

*2.5 Synthesis of ligand **1b***

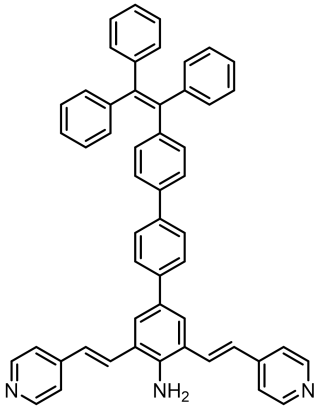

Compound **6** (100.0 mg, 0.13 mmol), 4-vinyl pyridine (54.9 mg, 0.52 mmol), $Pd(OAc)_2$ (2.2 mg, 0.01 mmol), $P(Ph)_3$ (10.5 mg, 0.04 mmol), NEt_3 (5 mL) were dissolved in dry DMF (40 mL) under nitrogen, and then the mixture solution was heated at 100 ℃ for 48 h. After cooling to room temperature, the mixture was filtered and the solvent was removed in vacuo. Then the mixture was extracted with CH_2Cl_2/H_2O three times, dried over anhydrous $MgSO_4$, filtered and removed to give a crude product. The crude product was further purified by flash column chromatography with CH_2Cl_2/CH_3OH (30:1, *v*/*v*) as the eluent to afford ligand **1b** as an orange solid (23.0 mg, 23.0%). M. P. 147–149 ℃. ^{1}H NMR (500 MHz, $CDCl_3$, 298 K) δ (ppm): 8.61 (d, 4H), 7.69–7.61 (m, 6H), 7.46–7.34 (m, 8H), 7.18–6.93 (m, 19H), 4.20 (s, 2H). ^{13}C NMR (125 MHz, $CDCl_3$, 298K) δ (ppm): 150.3, 144.5, 143.7, 143.7, 142.9, 141.9, 141.2, 140.5, 139.2, 139.1, 138.2, 131.9, 131.4, 131.4, 131.3, 129.0, 128.6, 127.8, 127.7, 127.6, 127.2, 126.8, 126.6, 126.5, 126.0, 124.0, 120.9. ESI-HRMS [**1b** + H]$^+$: calcd. for $[C_{52}H_{40}N_3]^+$ 706.3217, found 706.3317.

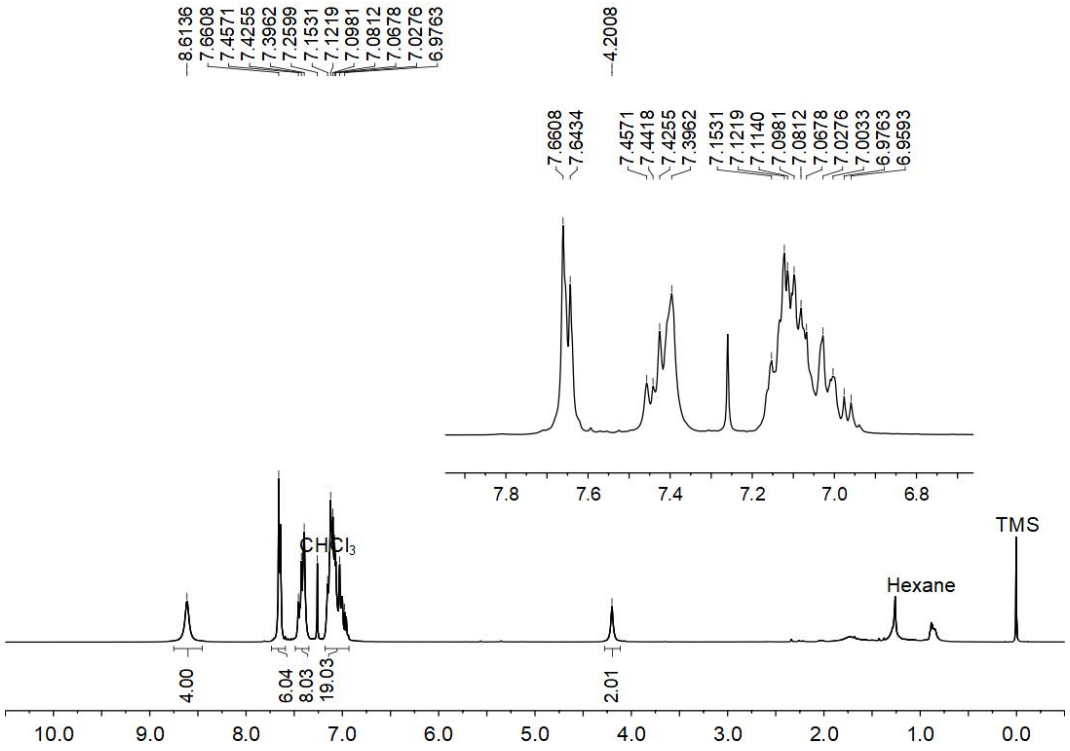

Figure S11. ^{1}H NMR spectrum (500 MHz, $CDCl_3$, 298 K) of ligand **1b**.

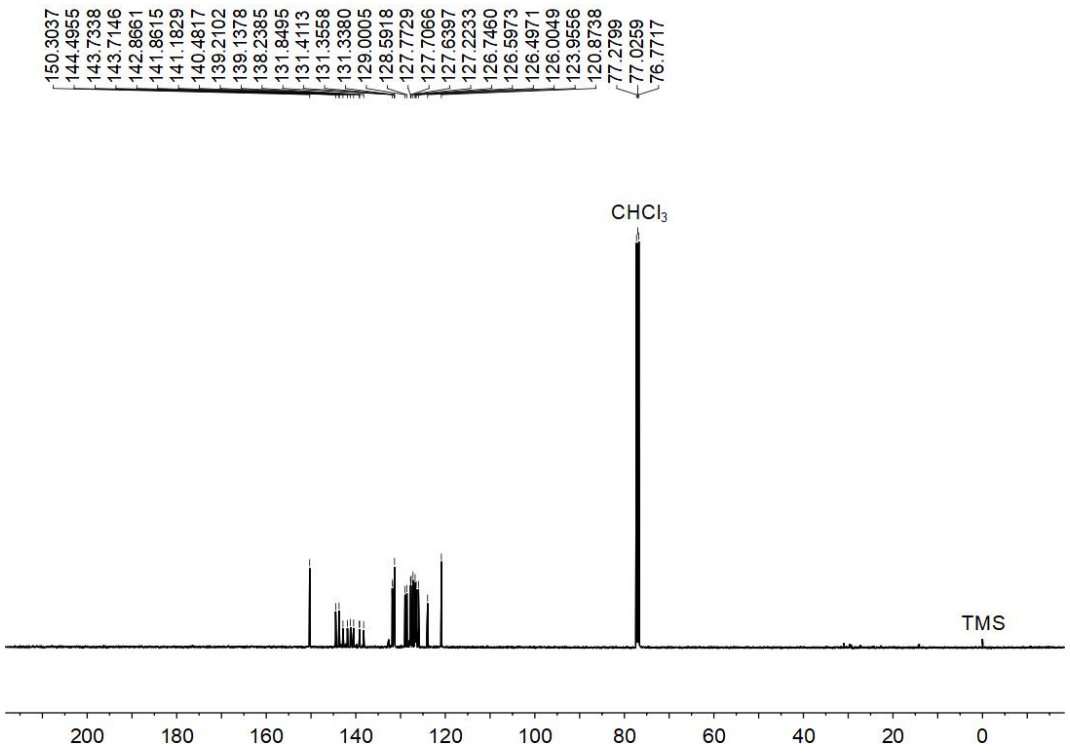

Figure S12. ^{13}C NMR spectrum (125 MHz, $CDCl_3$, 298 K) of ligand **1b**.

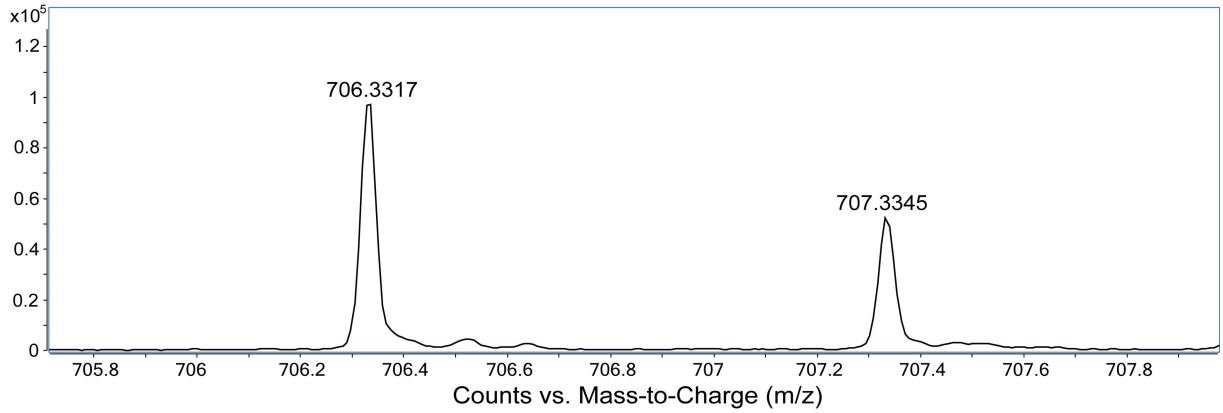

Figure S13. ESI-HRMS spectrum of ligand **1b**.

*2.6 Synthesis of ligand **1c***

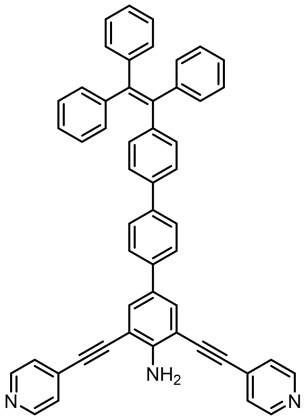

Compound **6** (100.0 mg, 0.13 mmol), 4-pyridylethyne hydrochloride (53.6 mg, 0.52 mmol), cuprous iodide (1.9 mg, 0.01 mmol), NEt_3 (5 mL), $Pd(PPh_3)_4$ (15.3 mg, 0.01 mmol) were dissolved in dry THF (40 mL) under nitrogen, and then the mixture solution was heated at 60 °C for 48 h. After cooling to room temperature, the mixture was filtered and the solvent was removed in vacuo. Then the mixture was extracted with CH_2Cl_2/H_2O three times, dried over anhydrous $MgSO_4$, filtered and removed to give a crude product. The crude product was further purified by flash column chromatography with CH_2Cl_2/CH_3OH (30:1, *v*/*v*) as the eluent to afford ligand **1c** as a yellow solid (20.0 mg, 20.0%). M. P. 153–155 °C. ^{1}H NMR (500 MHz, $CDCl_3$, 298 K) δ (ppm): 8.65 (d, 4H), 7.72 (d, J = 3.8 Hz, 2H), 7.62 (d, J = 8.7 Hz, 2H), 7.59 (dd, J = 8.4 Hz, 2H), 7.43–7.37 (m, 6H), 7.16–7.00 (m, 17H), 5.00 (s, 2H). ^{13}C NMR (125 MHz, $CDCl_3$, 298K) δ (ppm): 149.9, 148.6, 143.8, 143.7, 143.0, 141.2, 140.5, 139.4, 138.2, 138.0, 132.7, 132.11, 131.9, 131.4, 131.4, 131.0, 130.4, 127.9, 127.8, 127.7, 127.7, 127.3, 126.5, 126.0, 125.4, 107.1, 92.7, 89.8. ESI-HRMS [**1c** + H]$^+$: calcd. for $[C_{52}H_{36}N_3]^+$ 702.2904, found 702.4691.

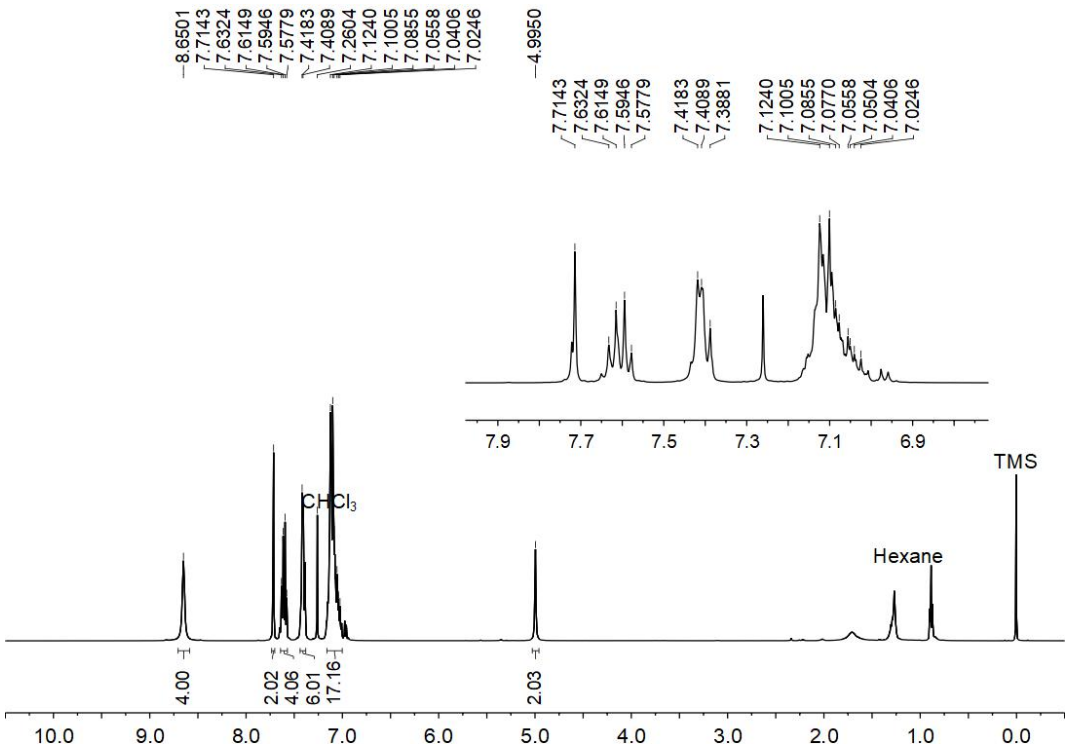

Figure S14. ^{1}H NMR spectrum (500 MHz, $CDCl_3$, 298K) of ligand **1c**.

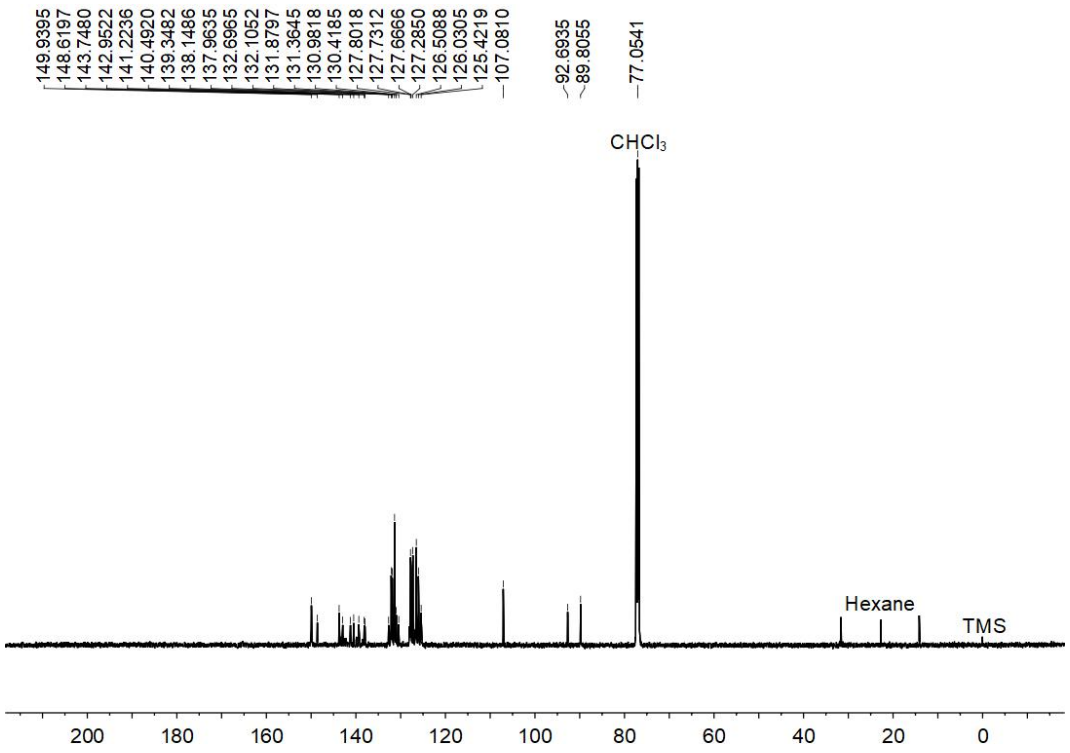

Figure S15. ^{13}C NMR spectrum (125 MHz, $CDCl_3$, 298K) of ligand **1c**.

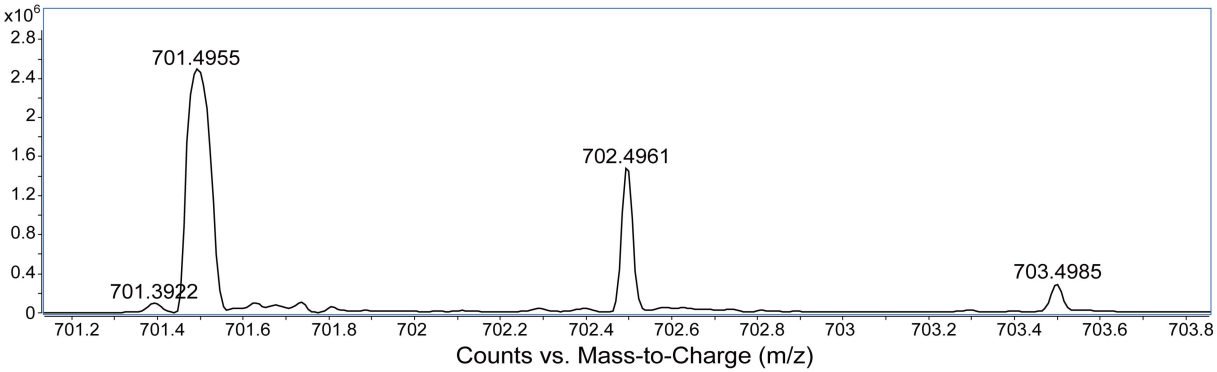

Figure S16. ESI-HRMS spectrum of ligand **1c**.

*2.7 Synthesis of compound **8***

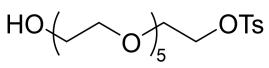

Compound **8** was synthesized according to literature procedure[S3]. The ^{1}H NMR of **8** matches well with the reported data. ^{1}H NMR (500 MHz, $CDCl_3$, 298K) δ (ppm): 7.79 (d, J = 8.3 Hz, 2H), 7.35 (d, J = 7.9 Hz, 2H), 4.22–4.11 (m, 2H), 3.73–3.53 (m, 24H), 2.45 (s, 3H)

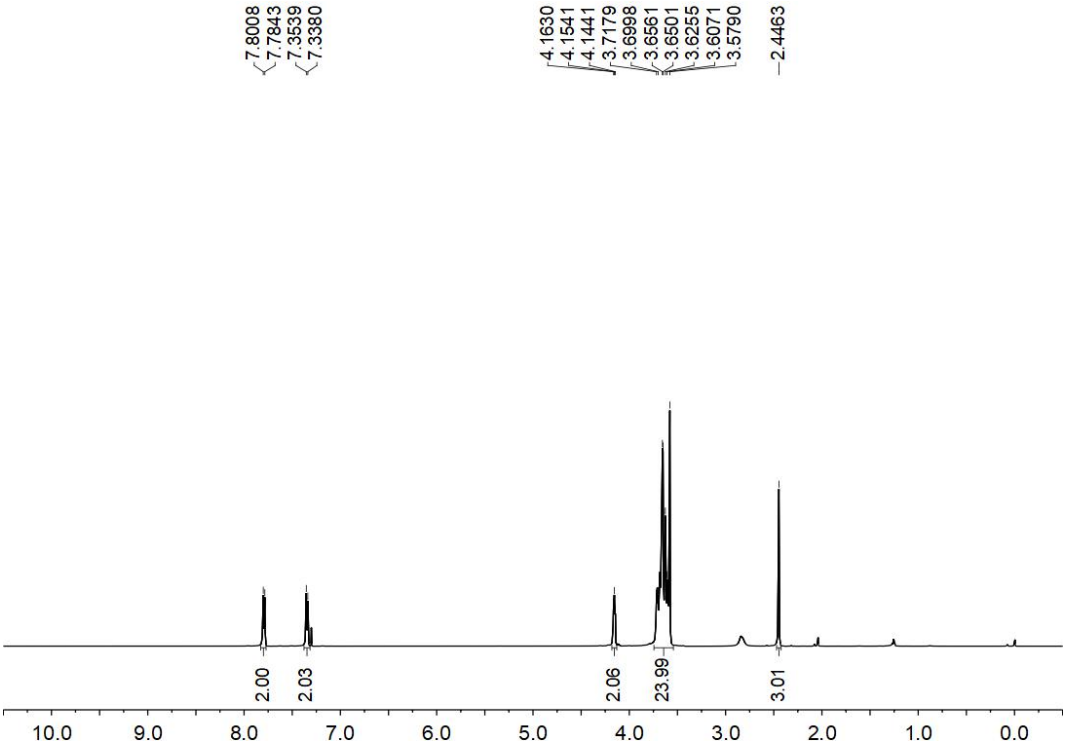

Figure S17. ^{1}H NMR spectrum (500 MHz, $CDCl_3$, 298 K) of compound **8**.

2.8 Synthesis of compound ***9***

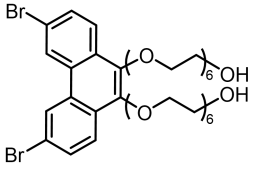

Compound **7**[S2] (0.5 g, 1.36 mmol), **8** (1.3 g, 2.99 mmol), K_2CO_3 (0.9 g, 6.80 mmol) were dissolved in dry DMF (100 mL) under nitrogen, and then the mixture solution was heated at 85 ℃ for 24 h. After cooling to room temperature, the solvent was removed in vacuo. Then the mixture was extracted with CH_2Cl_2/H_2O three times, dried over anhydrous $MgSO_4$, filtered and removed to give a crude product. The crude product was further purified by flash column chromatography with CH_2Cl_2/CH_3OH (20:1, *v*/*v*) as the eluent to afford compound **9** as a yellow oil (961.3 mg, 57.6%). ^{1}H NMR (500 MHz, $CDCl_3$, 298 K) δ (ppm): 8.54 (s, 2H), 8.14 (d, J = 8.8 Hz, 2H), 7.62 (d, J = 8.8, 2H), 4.35–4.24 (m, 4H), 3.78–3.74 (m, 4H), 3.69–3.45 (m, 40H). ^{13}C NMR (125 MHz, $CDCl_3$, 298K) δ (ppm): 141.9, 129.5, 127.9, 127.5, 124.2, 123.7, 119.5, 71.5, 69.6, 69.5, 69.5, 69.4, 69.4, 69.1, 60.5. ESI-HRMS [**9** + H]$^+$: calcd. for $[C_{38}H_{57}Br_2O_{14}]^+$ 895.2110, found 895.2735.

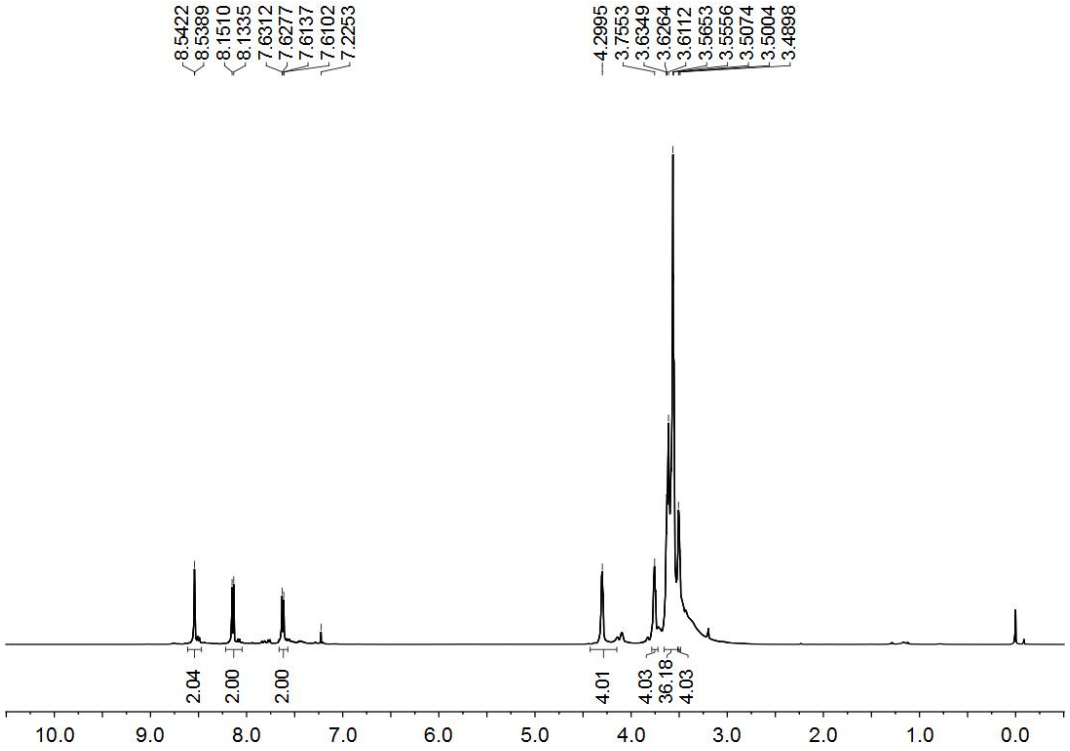

Figure S18. ^{1}H NMR spectrum (500 MHz, $CDCl_3$, 298 K) of compound **9**.

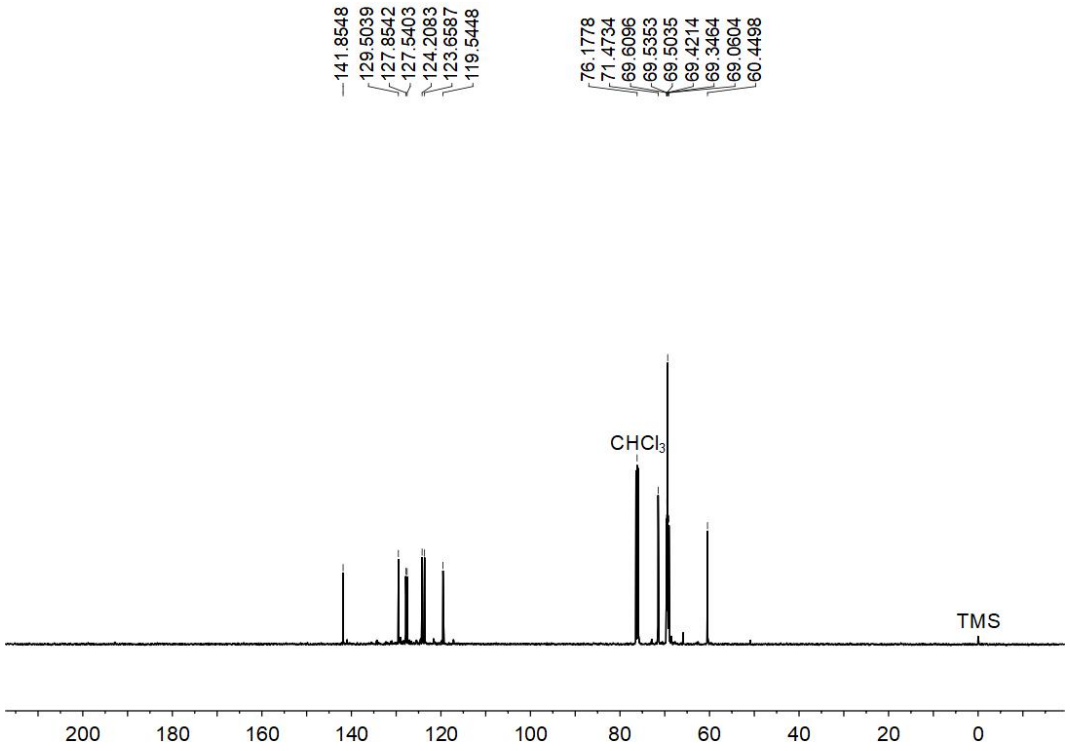

Figure S19. ^{13}C NMR spectrum (125 MHz, $CDCl_3$, 298 K) of compound **9**.

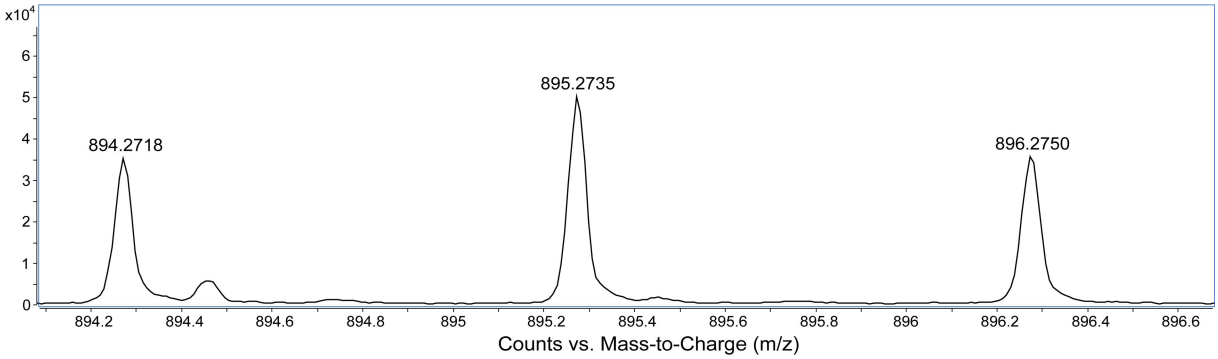

Figure S20. ESI-HRMS spectrum of compound **9**.

*2.9 Synthesis of compound **10***

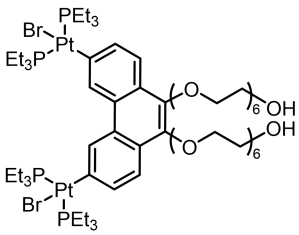

Compound **9** (200.0 mg, 0.22 mmol) and $Pt(PEt_3)_4$[S3] (293.3 mg, 0.44 mmol) were dissolved in dry toluene (50 mL) by syringe under nitrogen, and then the mixture solution was stirred at 90 ℃ for 72 h. After cooling to room temperature, the solvent was removed in vacuo to give a crude product. The crude product was further purified by flash column chromatography with CH_2Cl_2/CH_3OH (30:1, *v*/*v*) as the eluent to afford compound **10** as a yellow oil (445.9 mg, 91.1%). ^{1}H NMR (500 MHz, $CDCl_3$, 298 K) δ (ppm): 8.46 (s, 2H), 7.76 (d, J = 8.1 Hz, 2H), 7.56 (d, J = 7.9 Hz, 2H), 4.38–4.32 (m, 4H), 3.94–3.82 (m, 4H), 3.75–3.62 (m, 36H), 3.60–3.56 (m, 4H), 1.72–1.56 (m, 24H), 1.12–0.98 (m, 36H). ^{13}C NMR (125 MHz, $CDCl_3$, 298K) δ (ppm): 141.1, 136.5, 135.4, 129.3, 128.3, 124.7, 120.6, 72.6, 72.1, 70.8, 70.7, 70.7, 70.6, 70.5, 70.3, 61.7, 14.2, 14.1, 13.9, 13.6, 13.4, 13.3, 7.8, 7.8. ESI-HRMS [**10**

+ Na]$^+$: calcd. for [$C_{62}H_{116}Br_2O_{14}P_4Pt_2Na$]$^+$ 1769.4773, found 1769.5153.

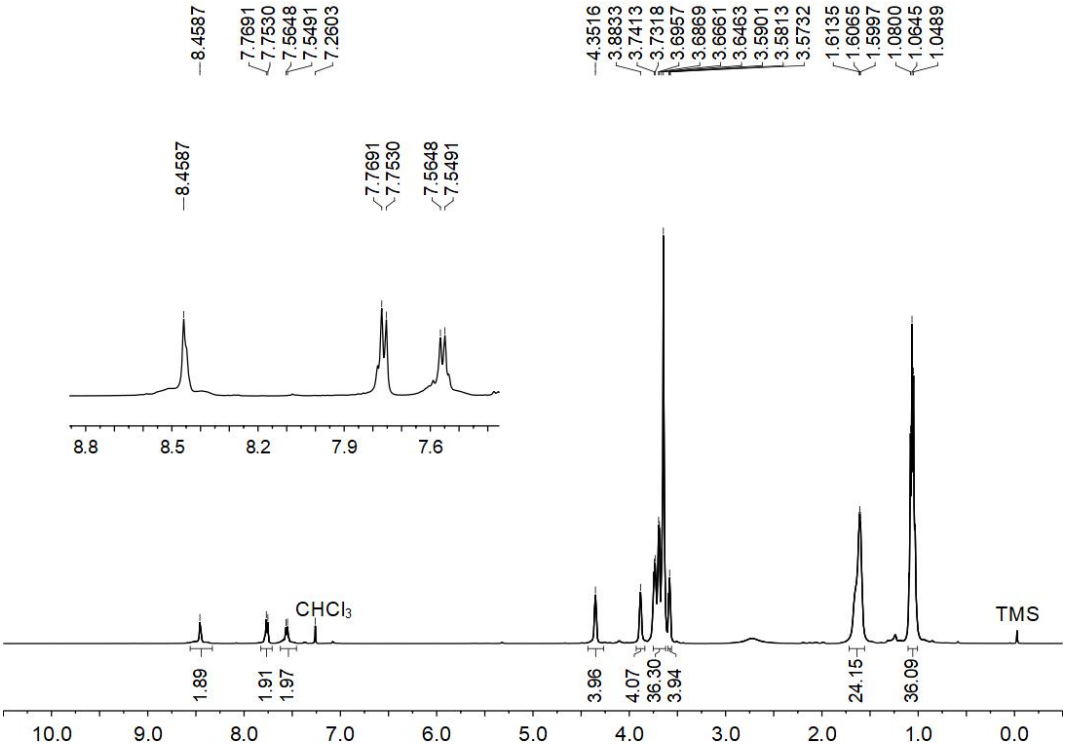

Figure S21. ^{1}H NMR spectrum (500 MHz, $CDCl_3$, 298 K) of compound **10**.

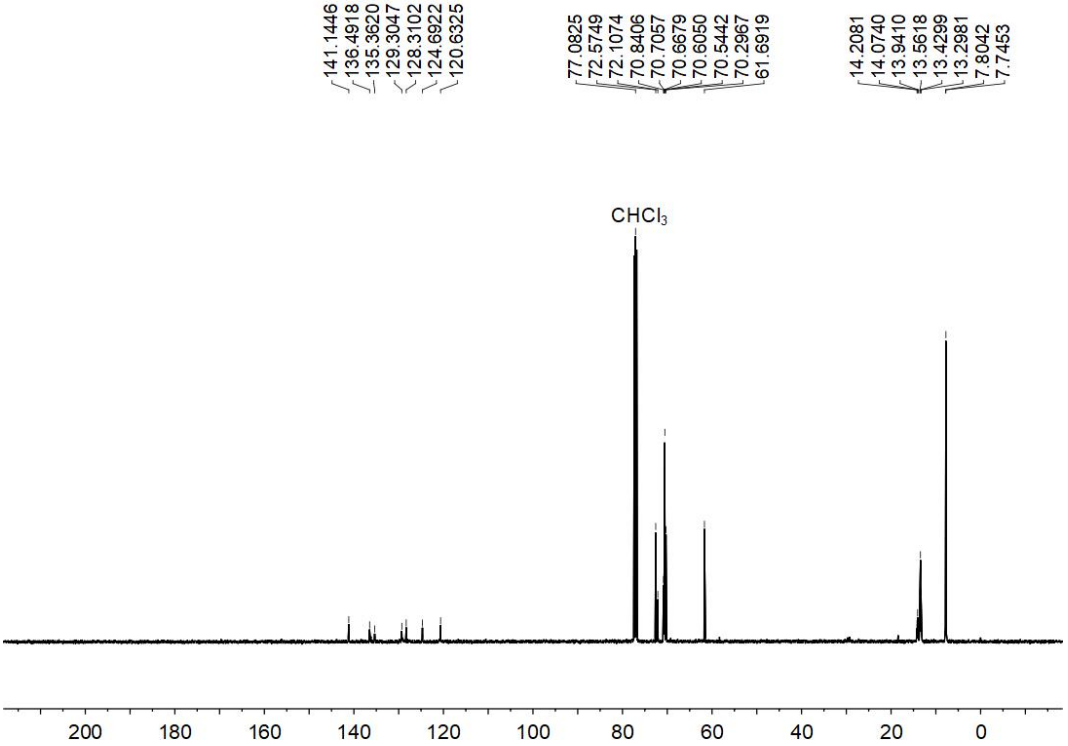

Figure S22. ^{13}C NMR spectrum (125 MHz, $CDCl_3$, 298 K) of compound **10**.

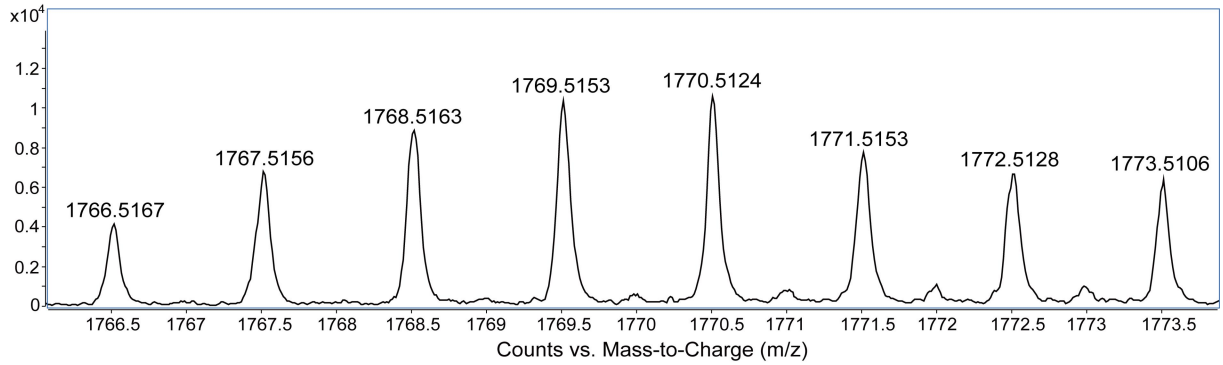

Figure S23. ESI-HRMS spectrum of compound **10**.

*2.10 Synthesis of acceptor **2***

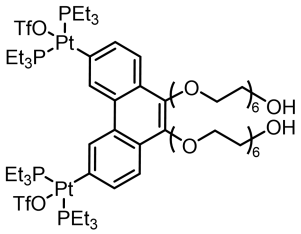

Compound **10** (100.0 mg, 0.06 mmol) and silver trifluoromethane sulfonate (87.7 mg, 0.30 mmol) were dissolved in dry CH_2Cl_2 (8 mL), and then the mixture solution was stirred at room temperature for 8 h under nitrogen. After then, the mixture was filtered and the solvent was removed in vacuo to afford acceptor **2** as a brown oil (92.4 mg, 92.3%). ^{1}H NMR (500 MHz, CD_2Cl_2, 298 K) δ (ppm): 8.34 (s, 2H), 7.76 (d, J = 7.5 Hz, 2H), 7.56 (d, J = 8.2 Hz, 2H), 4.52–4.28 (m, 4H), 3.98–3.85 (m, 4H), 3.86–3.68 (m, 36H), 3.66–3.58 (m, 4H), 1.71–1.48 (m, 24H), 1.15–0.95 (m, 36H). ^{13}C NMR (125 MHz, CD_2Cl_2, 298K) δ (ppm): 141.6, 135.6, 128.5, 128.3, 125.2, 121.9, 121.0, 119.3, 72.8, 71.7, 71.0, 70.9, 70.4, 70.3, 70.3, 70.1, 69.8, 69.7, 69.5, 14.0, 13.8, 13.7, 12.8, 7.6. ^{31}P{^{1}H} NMR (202 MHz, CD_2Cl_2, 298 K) δ (ppm): 19.51 ppm (s, ^{195}Pt satellites $^1J_{Pt-P}$ = 2831.4 Hz). ESI-TOF-MS [**2** – OTf]$^+$: calcd. for $[C_{63}H_{116}F_3O_{17}P_4Pt_2S]^+$ 1746.6110, found 1746.6113.

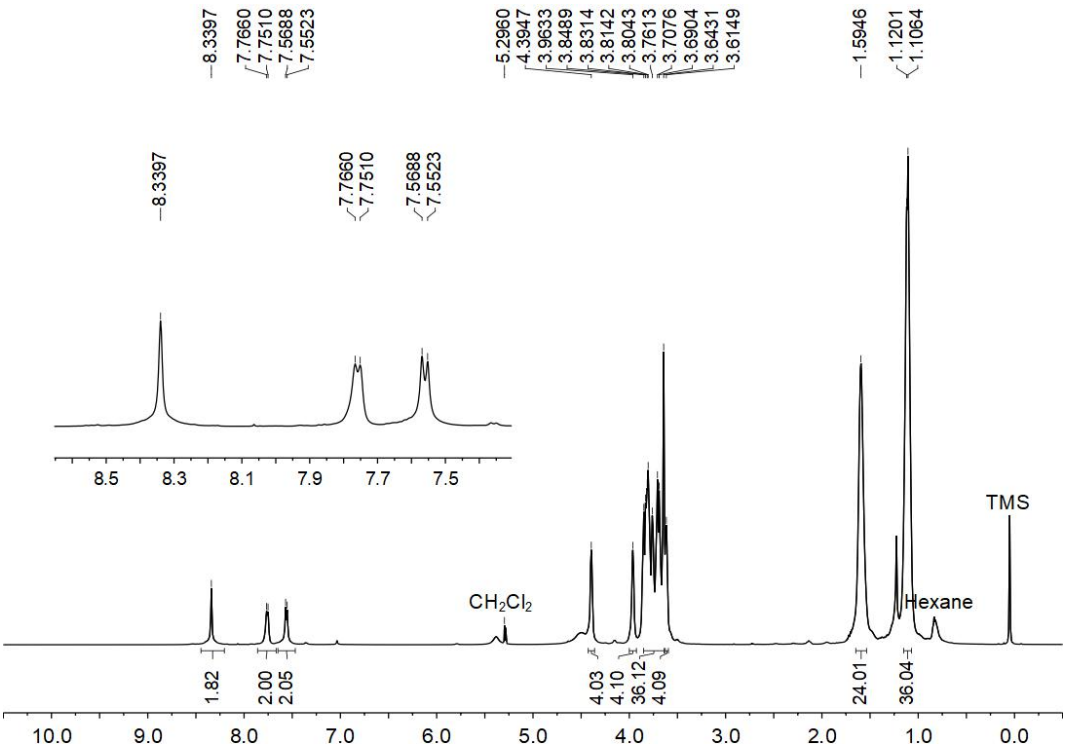

Figure S24. ^{1}H NMR spectrum (500 MHz, CD_2Cl_2, 298 K) of acceptor **2**.

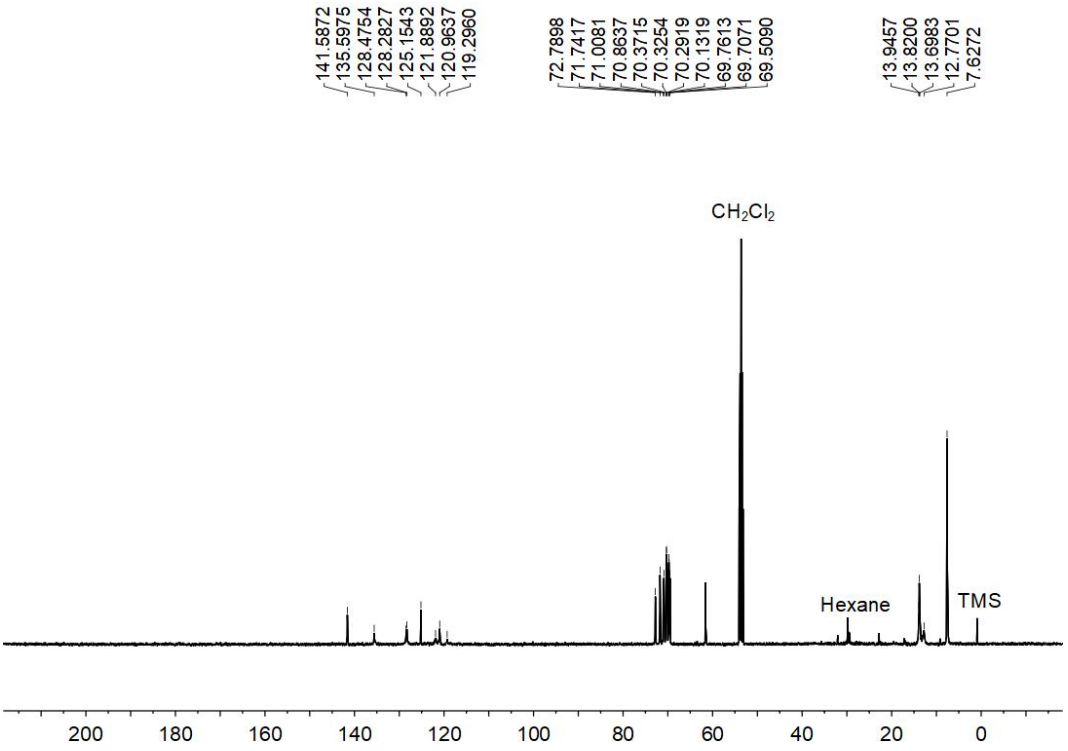

Figure S25. ^{13}C NMR spectrum (125 MHz, CD_2Cl_2, 298 K) of acceptor **2**.

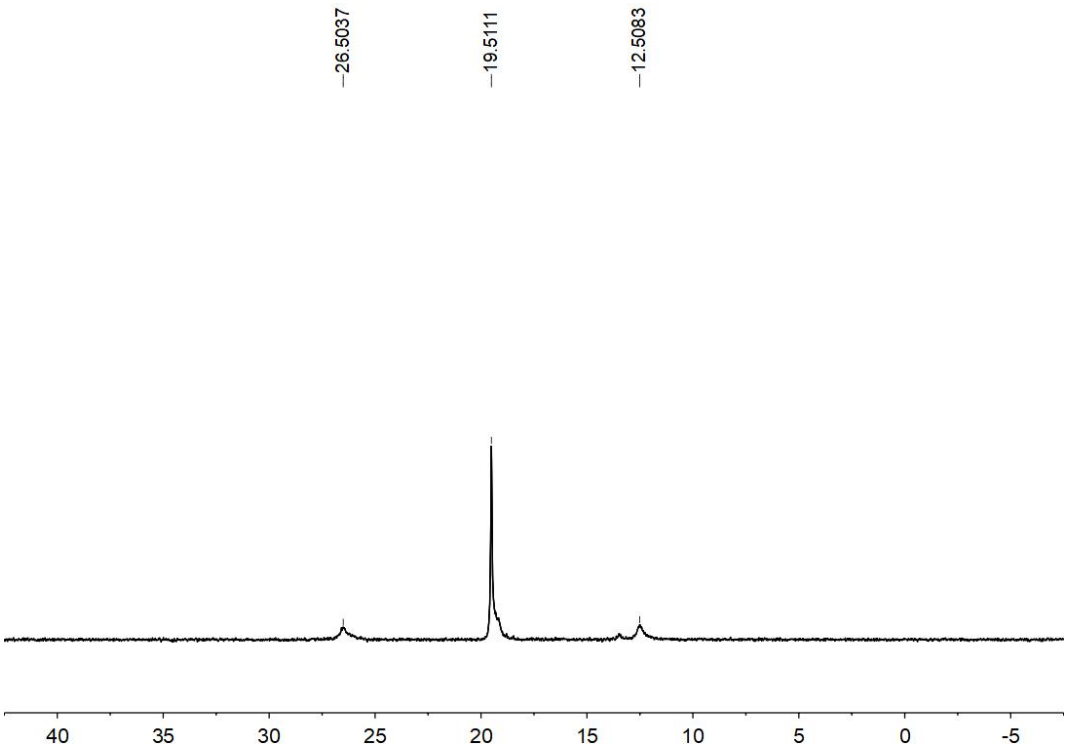

Figure S26. $^{31}P\{^{1}H\}$ NMR spectrum (202 MHz, CD_2Cl_2, 298 K) of acceptor **2**.

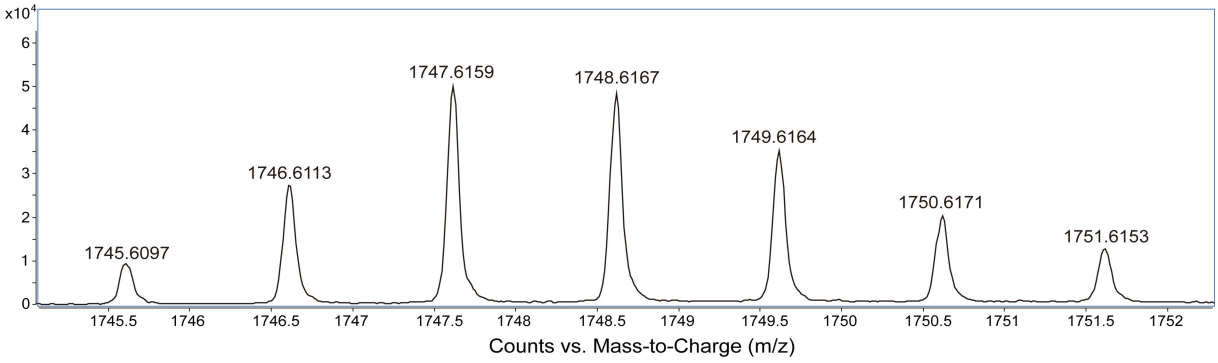

Figure S27. ESI-HRMS spectrum of acceptor **2**.

*2.11 Synthesis of metallacycle **3a***

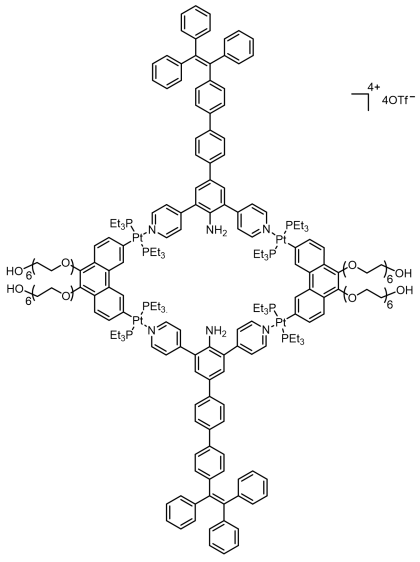

Compound **1a** (5.17 mg, 7.90 μmol) and **2** (15.00 mg, 7.90 μmol) were dissolved in dry CH_3OH (2.0 mL), and then the mixture solution was stirred at 55 °C for 12 h. After cooling to room temperature, diethyl ether (10 mL) was added to the above solution to obtain the desired product **3a** (15.93 mg, 79.4 %) as a pale yellow solid precipitate. ^{1}H NMR (500 MHz, CD_2Cl_2) δ (ppm): 9.09 (d, J = 5.7 Hz, 2H), 8.65 (d, J = 6.0 Hz, 6H), 8.37 (d, J = 5.0 Hz, 2H), 7.92 (d, J = 8.2 Hz, 4H), 7.80 (d, J = 5.4 Hz, 2H), 7.70–7.51 (m, 18H), 7.36 (t, J = 10.5 Hz, 4H), 7.10–6.91 (m, 40H), 4.36 (s, 8H), 3.91 (s, 8H), 3.84–3.45 (m, 80H), 1.33 (s, 48H), 1.15–0.96 (m, 72H). $^{31}P\{^{1}H\}$ NMR (202

MHz, CD_2Cl_2, 298 K) δ (ppm): 12.51 ppm (s, ^{195}Pt satellites, $^1J_{Pt-P}$ = 2685.2 Hz). ESI-TOF-MS [**3a**–3OTf+3Na–3H]$^{3+}$: calcd. for $[C_{221}H_{299}F_3N_6Na_3O_{31}P_8Pt_4S]^{3+}$ 1574.94, found 1574.46.

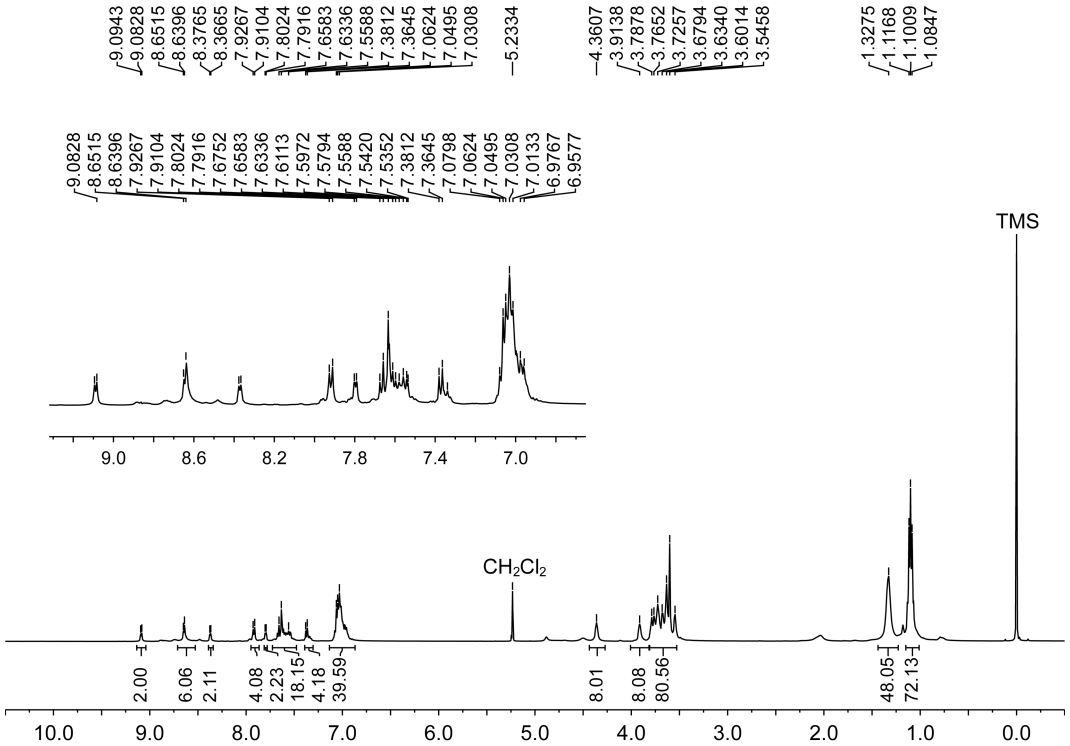

Figure S28. ^1H NMR spectrum (500 MHz, CD_2Cl_2, 298 K) of metallacycle **3a**.

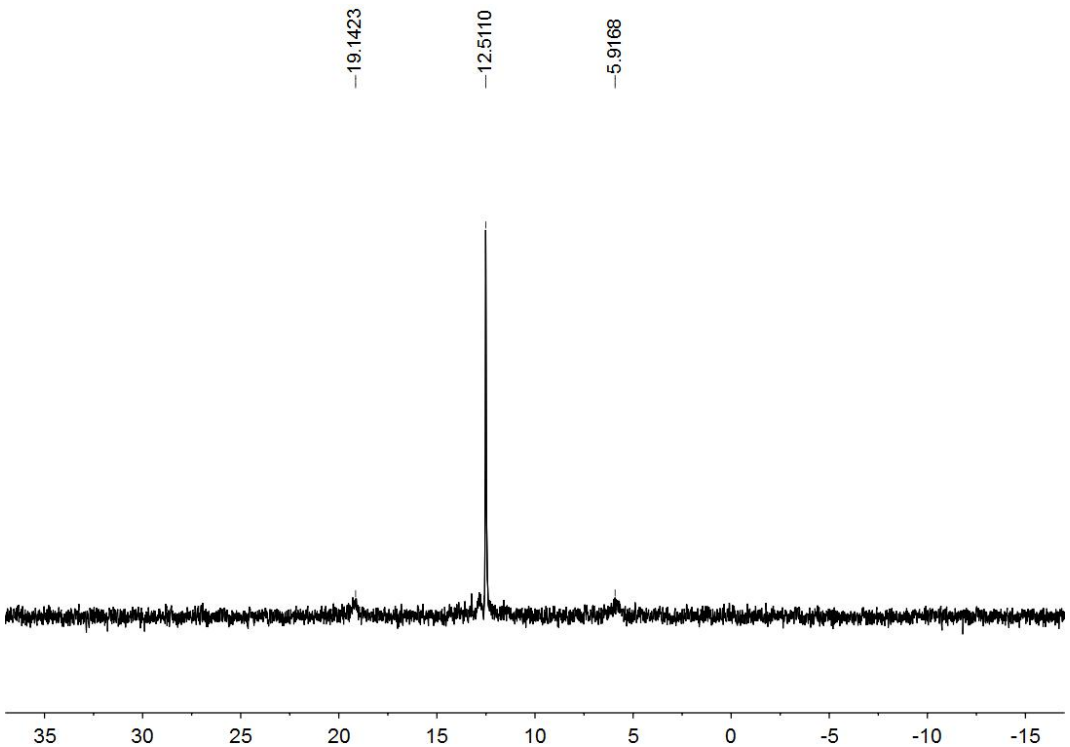

Figure S29. $^{31}P\{^1H\}$ NMR spectrum (202 MHz, CD_2Cl_2, 298 K) of metallacycle **3a**.

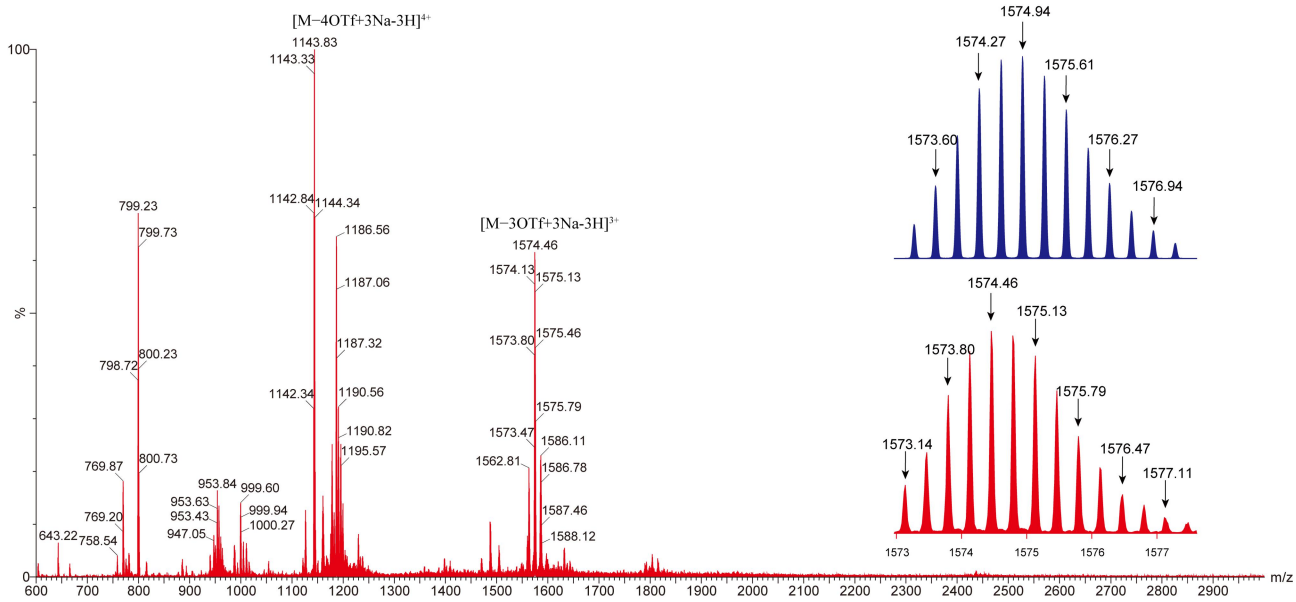

Figure S30. ESI-TOF-MS spectra of metallacycle **3a** [**3a**–3OTf+3Na–3H]$^{3+}$. Inset: calculated (blue) and experimental (red).

*2.12 Synthesis of metallacycle **3b***

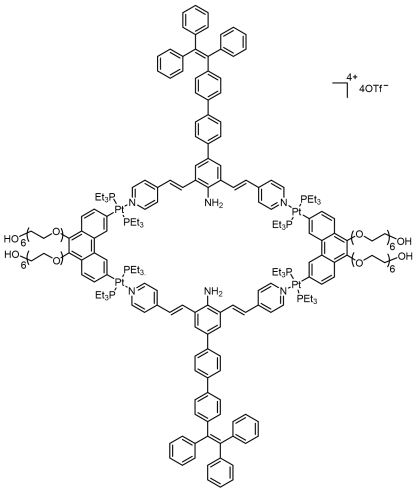

Compound **1b** (5.58 mg, 7.90 μmol) and **2** (15.00 mg, 7.90 μmol) were dissolved in dry CH_3OH (2.0 mL), and then the mixture solution was stirred at 55 °C for 12 h. After cooling to room temperature, diethyl ether (10 mL) was added to the above solution to obtain the desired product **3b** (17.29 mg, 84.3%) as an orange solid precipitate. ^{1}H NMR (500 MHz, CD_2Cl_2, 298 K) δ (ppm): 8.72 (d, J = 5.8 Hz, 2H), 8.49 (s, 4H), 8.44 (d, J = 5.5 Hz, 4H), 8.30 (d, J = 5.4 Hz, 2H), 7.96 (dd, J = 20.1, 12.0 Hz, 8H), 7.84 (s, 2H), 7.70–7.54 (m, 14H), 7.49 (d, J = 5.3 Hz, 2H), 7.39 (d, J = 8.1 Hz, 4H), 7.18–6.88 (m, 44H), 4.32 (s, 8H), 3.85 (s, 8H), 3.76–3.27 (m, 80H), 1.30 (s, 48H), 1.16–1.02 (m, 72H). ^{31}P{^{1}H} NMR (202 MHz, CD_2Cl_2, 298 K) δ (ppm): 13.26 ppm (s, ^{195}Pt satellites, $^1J_{Pt-P}$ = 2698.2 Hz). ESI-TOF-MS [**3b**–3OTf+3Na–3H]$^{3+}$: calcd. for [$C_{229}H_{307}F_3N_6Na_3O_{31}P_8Pt_4S$]$^{3+}$ 1609.62, found 1609.49.

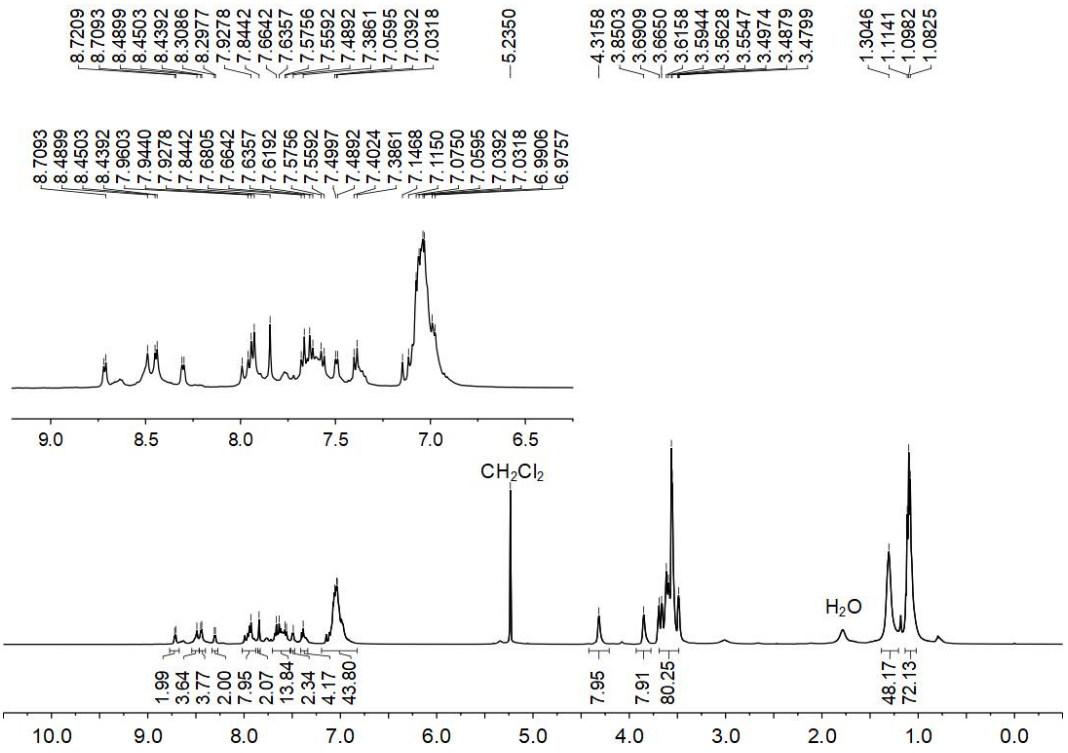

Figure S31. ^{1}H NMR spectrum (500 MHz, CD_2Cl_2, 298 K) of metallacycle **3b**.

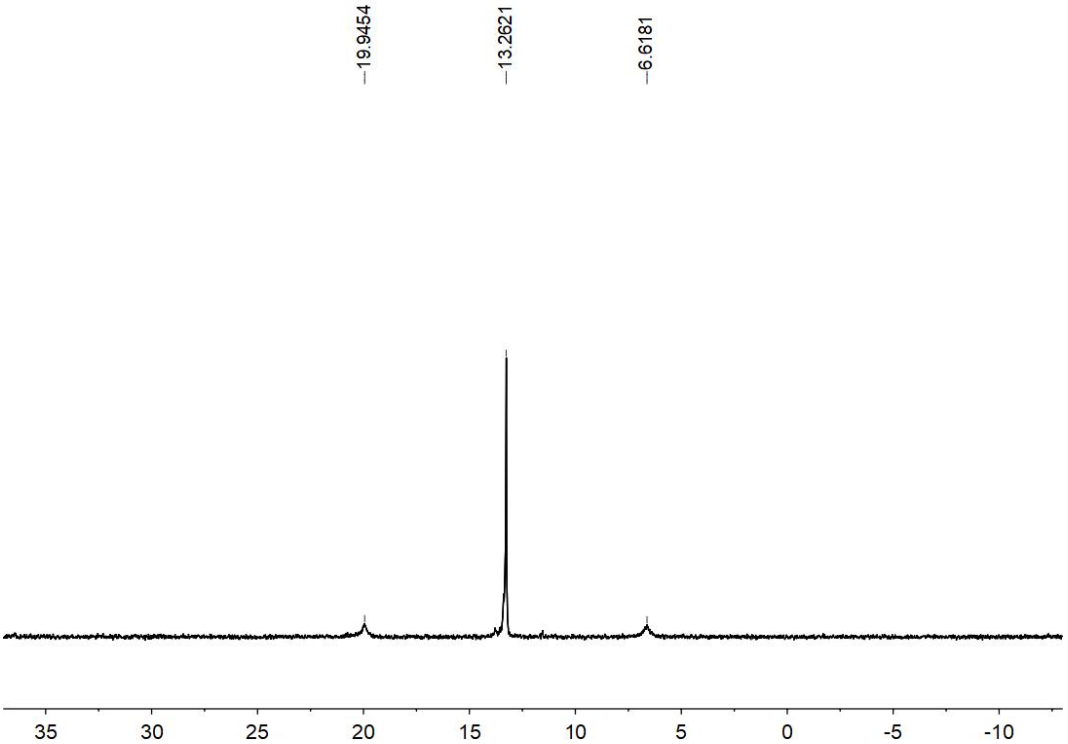

Figure S32. ^{31}P{^{1}H} NMR spectrum (202 MHz, CD_2Cl_2, 298 K) of metallacycle **3b**.

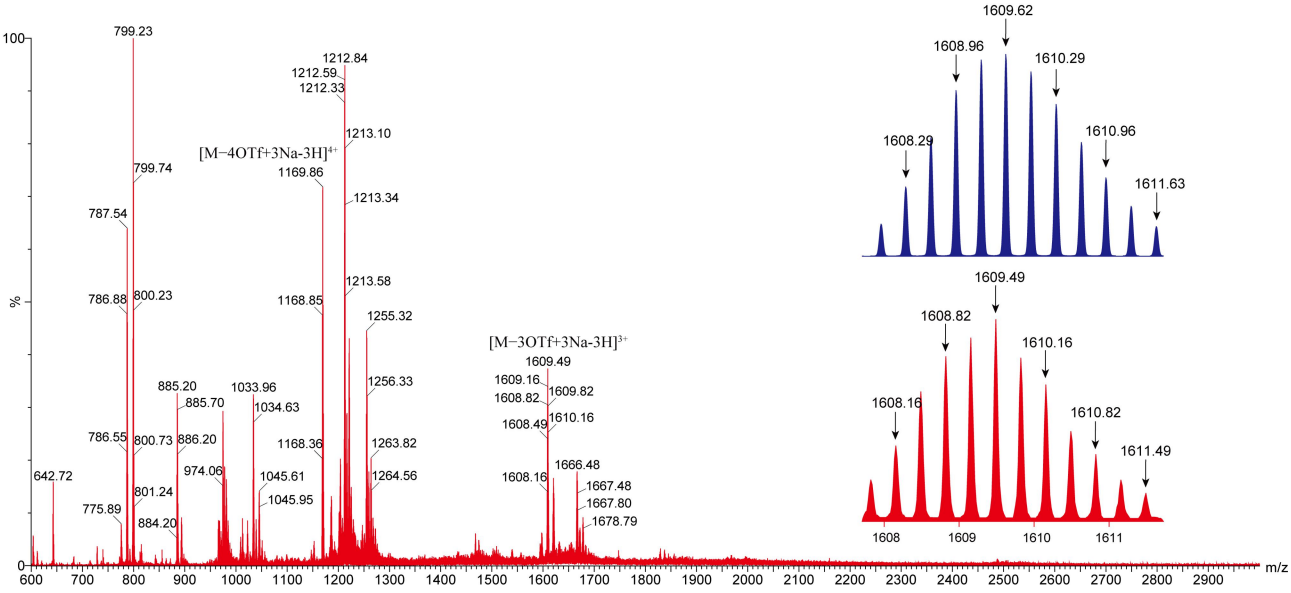

Figure S33. ESI-TOF-MS spectra of metallacycle **3b** [**3b**–3OTf+3Na–3H]$^{3+}$. Inset: calculated (blue) and experimental (red).

*2.13 Synthesis of metallacycle **3c***

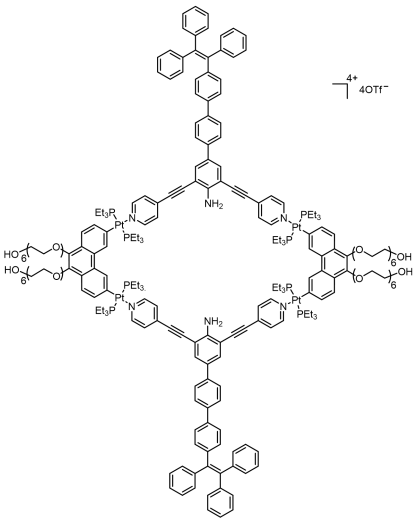

Compound **1c** (5.54 mg, 7.90 μmol) and **2** (15.00 mg, 7.90 μmol) were dissolved in dry CH_3OH (2.0 mL), and then the mixture solution was stirred at 55 °C for 12 h. After cooling to room temperature, diethyl ether (10 mL) was added to the above solution to obtain the desired product **3c** (16.64 mg, 81.2 %) as a deep yellow solid precipitate. ^{1}H NMR (500 MHz, CD_2Cl_2, 298 K) δ (ppm): 8.82 (d, J = 5.6 Hz, 2H), 8.58 (d, J = 5.5 Hz, 4H), 8.46 (s, 2H), 8.07 (d, J = 5.5 Hz, 2H), 7.94 (d, J = 8.2 Hz, 4H), 7.79 (s, 4H), 7.68 (d, J = 5.5 Hz, 4H), 7.59 (dd, J = 15.9, 9.3 Hz, 10H), 7.38 (d, J = 8.1 Hz, 6H), 7.03 (m, 40H), 4.32 (s, 8H), 3.85 (s, 8H), 3.74–3.39 (m, 80H), 1.30 (s, 48H), 1.16–0.98 (m, 72H). ^{31}P{^{1}H} NMR (202 MHz, CD_2Cl_2, 298 K) δ (ppm): 13.04 ppm (s, ^{195}Pt satellites, $^1J_{Pt-P}$ = 2680.6 Hz). ESI-TOF-MS [**3c**–3OTf]$^{3+}$: calcd. for $[C_{229}H_{302}F_3N_6O_{31}P_8Pt_4S]^{3+}$ 1583.95, found 1583.83.

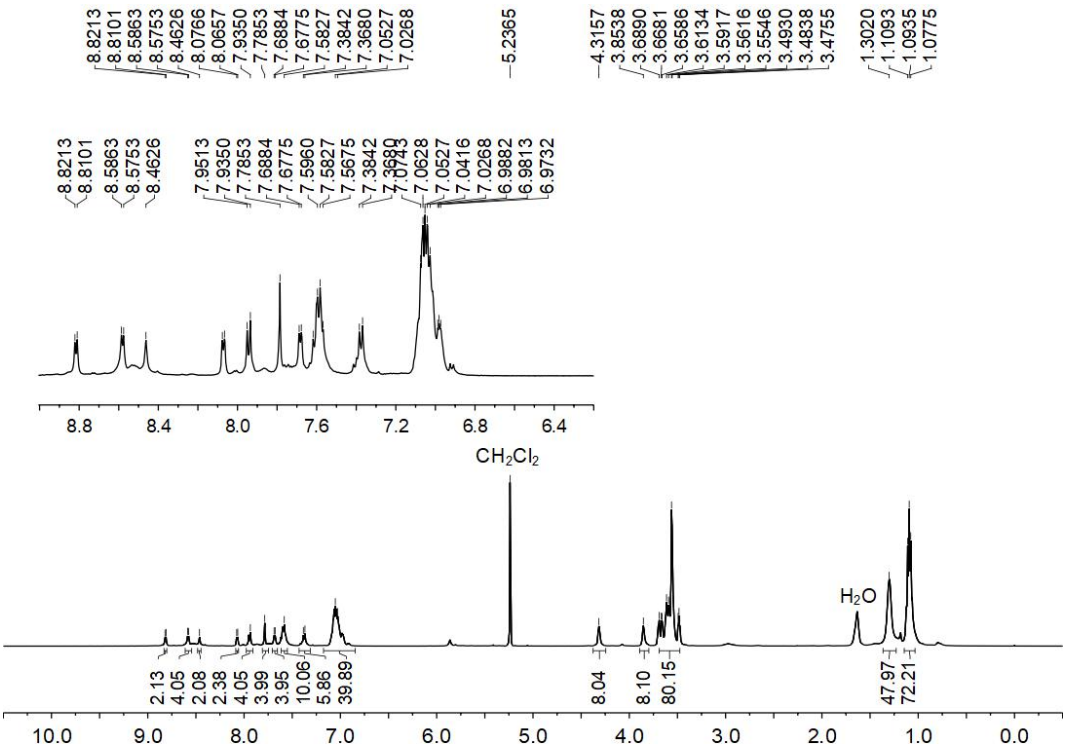

Figure S34. ^{1}H NMR spectrum (500 MHz, CD_2Cl_2, 298 K) of metallacycle **3c**.

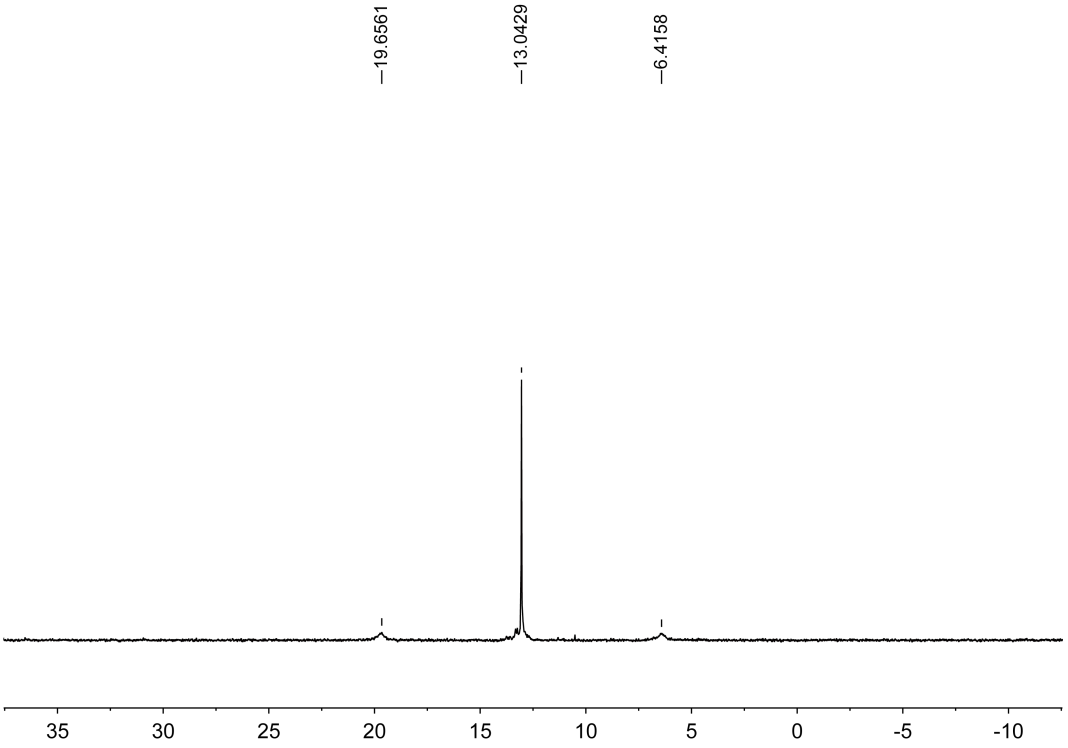

Figure S35. ^{31}P{^{1}H} NMR spectrum (202 MHz, CD_2Cl_2, 298 K) of metallacycle **3c**.

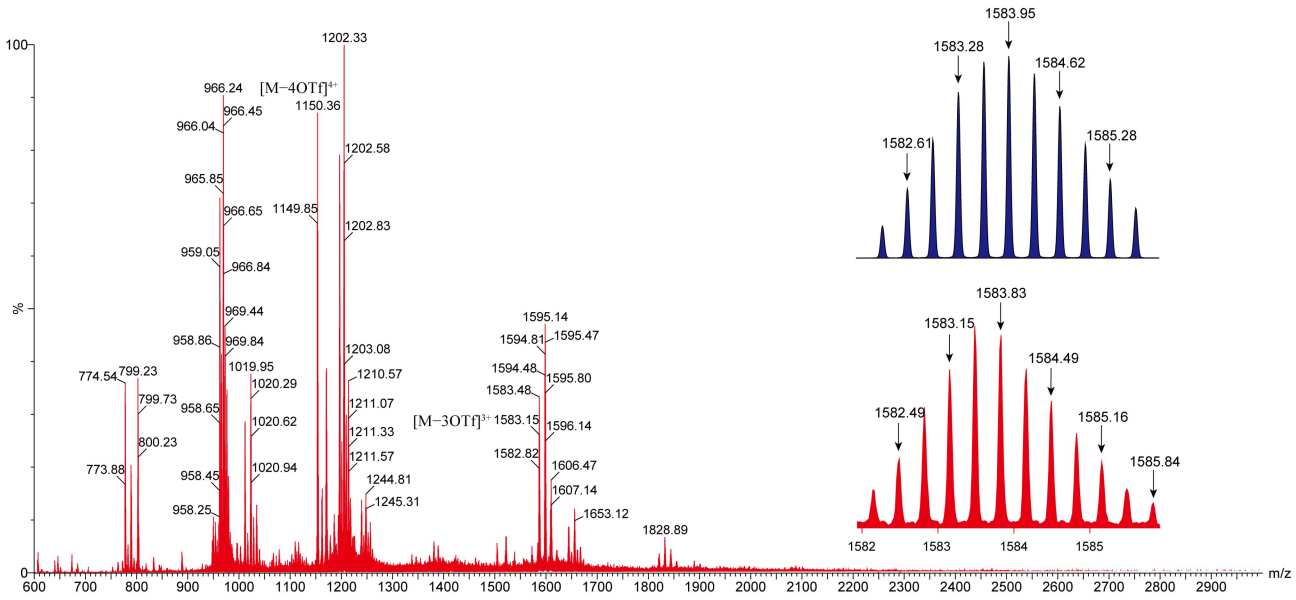

Figure S36. ESI-TOF-MS spectra of metallacycle **3c** [**3c**–3OTf]$^{3+}$. Inset: calculated (blue) and experimental (red).

*3. DFT calculations of ligands **1a-1c** and metallacycles **3a-3c**.*

Table S1. TD-PBE0 results on ground state

Compound	λ / nm	f	MO transition
ligand **1a**	369.1	1.124	HOMO → LUMO (89.7%)
ligand **1b**	418.7	0.417	HOMO → LUMO (78.4%) HOMO−1 → LUMO (19.7%)
ligand **1c**	421.0	0.492	HOMO → LUMO (77.3%) HOMO−1 → LUMO (21.0%)
metallacycle **3a**	448.8	0.014	HOMO → LUMO (54.9%) HOMO−1 → LUMO+1 (21.9%) HOMO → LUMO+1 (15.7%)
metallacycle **3b**	510.5	0.049	HOMO−1 → LUMO (70.6%) HOMO → LUMO + 1 (11.2%)
metallacycle **3c**	527.9	0.003	HOMO−1 → LUMO (45.3%) HOMO → LUMO + 1 (28.2%)

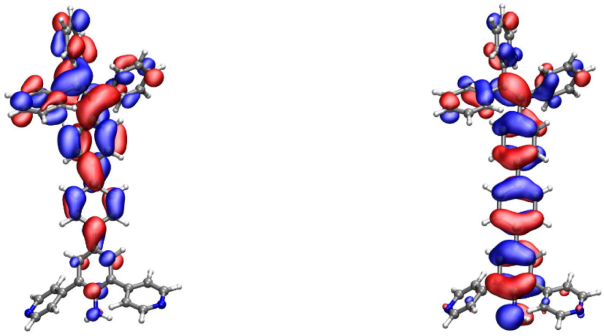

Figure S37. Frontier molecular orbitals of ligand **1a** at the ground state.

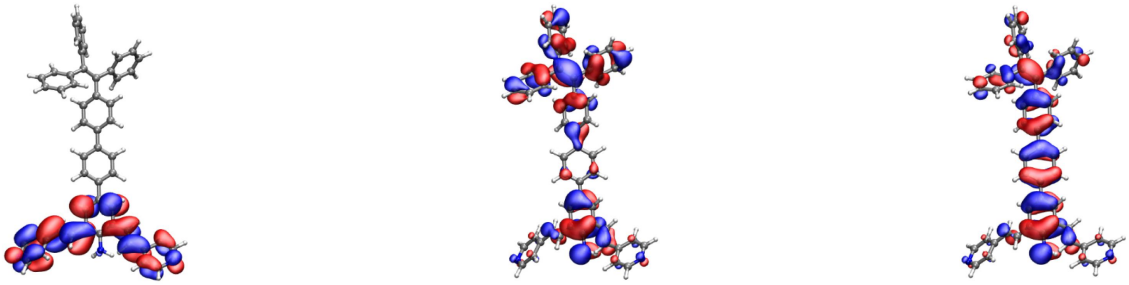

Figure S38. Frontier molecular orbitals of ligand **1b** at the ground state.

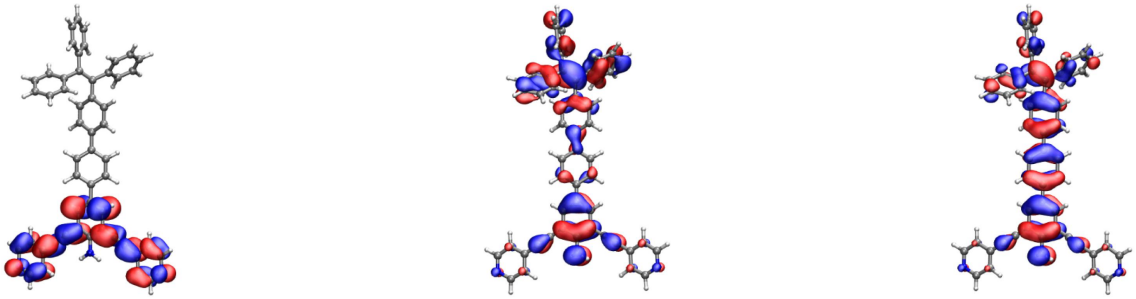

Figure S39. Frontier molecular orbitals of ligand **1c** at the ground state.

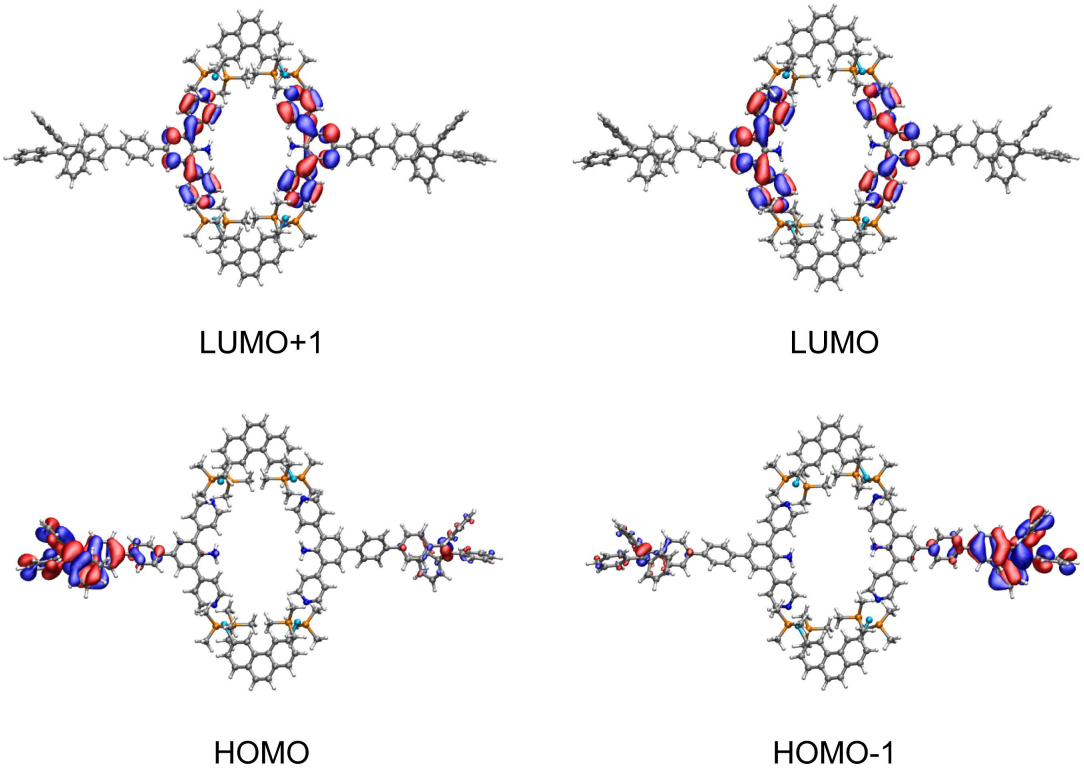

Figure S40. Frontier molecular orbitals of metallacycle **3a** at the ground state.

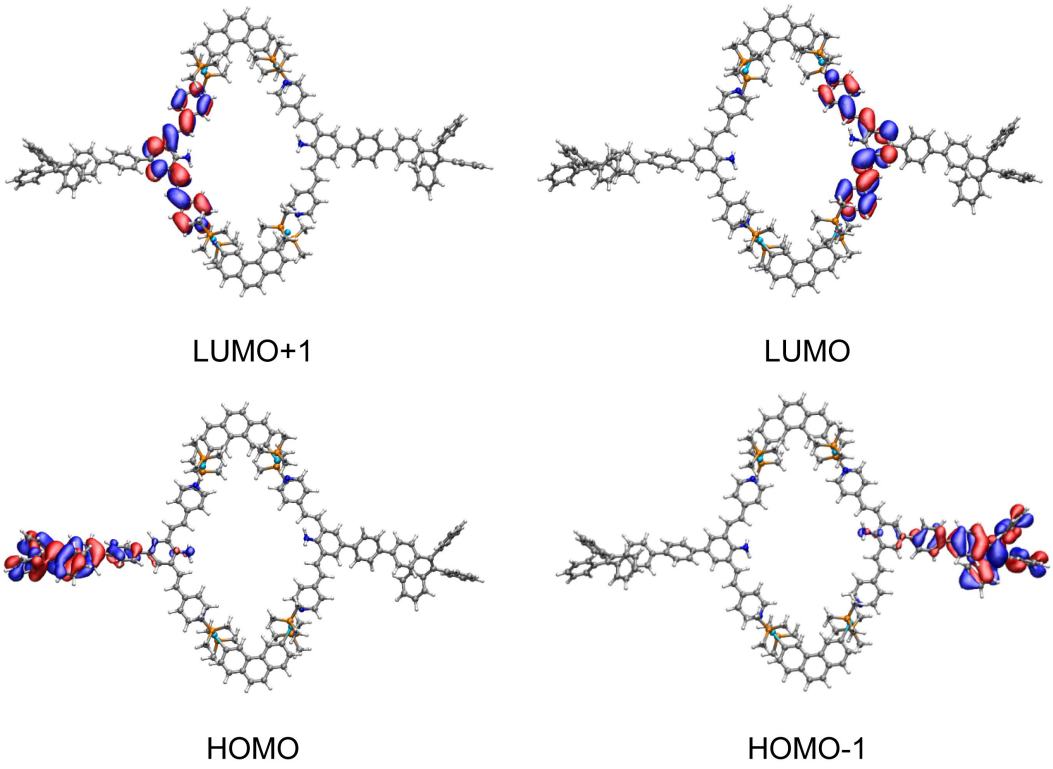

Figure S41. Frontier molecular orbitals of metallacycle **3b** at the ground state.

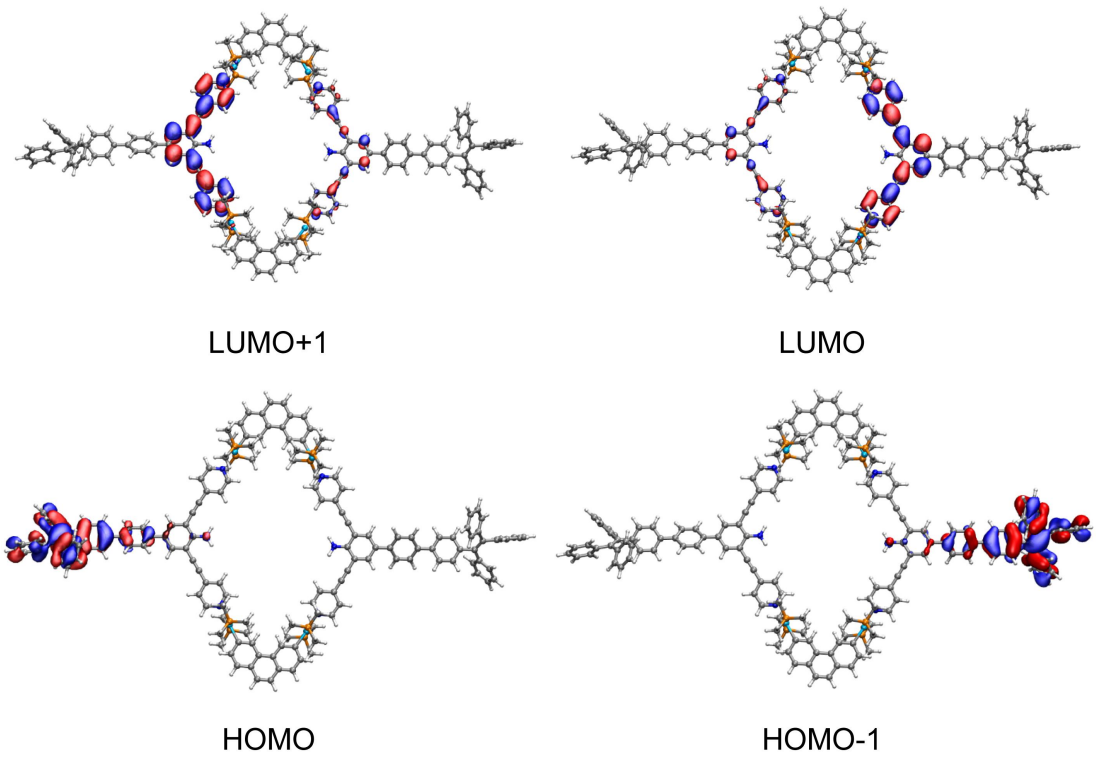

Figure S42. Frontier molecular orbitals of metallacycle **3c** at the ground state.

*4. Optical characterization data of metallacycles **3a-3c** in different solvents*

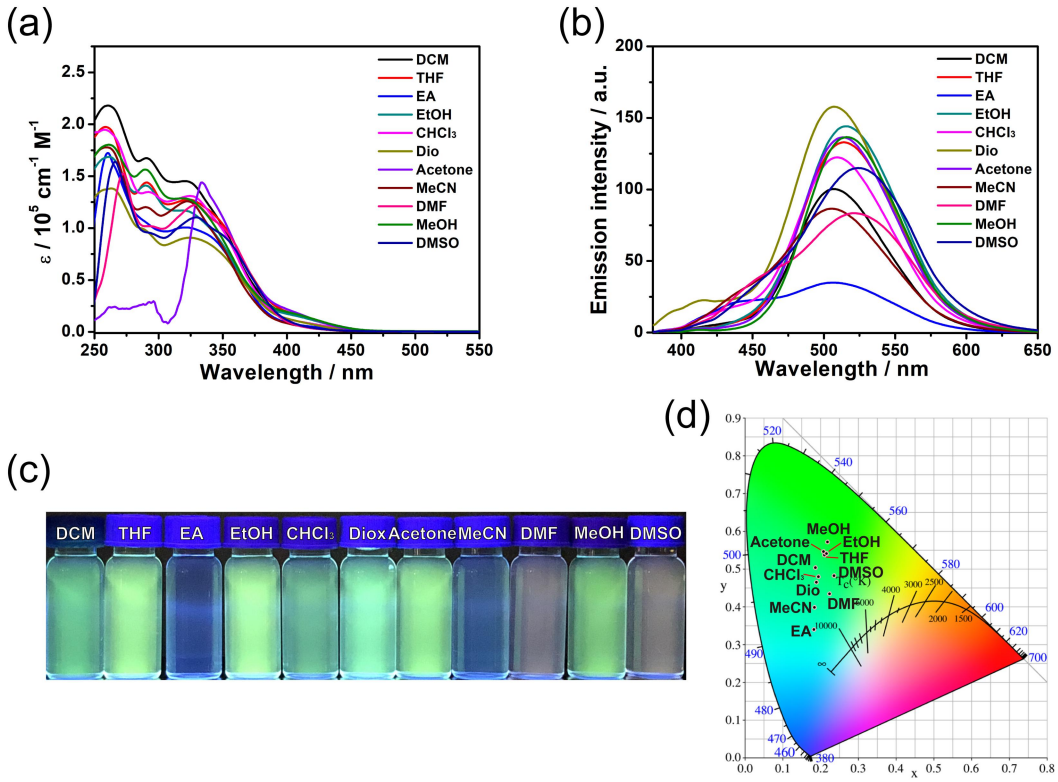

Figure S43. (a) Absorption and (b) emission spectral profiles of metallacycle **3a** in different solvents. (c) Images of metallacycle **3a** under UV lamp in different solvents. (d) CIE chromaticity coordinates of metallacycle **3a** in different solvents (c = 10.0 μM, λ_{ex} = 365 nm).

Table S2. Molar absorption coefficients, emission spectral data, CIE chromaticity coordinates and quantum yields of metallacycle **3a** in different solvents (c = 10.0 μM, λ_{ex} = 365 nm).

Solvents	λ_{ab} / nm [$\varepsilon \times 10^5$, $cm^{-1}\ M^{-1}$]	λ_{em} / nm	CIE	Φ (%)
CH_2Cl_2	292 [1.696], 324 [1.457]	507	(0.19, 0.50)	0.7
THF	290 [1.486], 324 [1.283]	514	(0.21, 0.54)	1.1
EA	322 [1.013]	450, 505	(0.18, 0.34)	0.4
C_2H_5OH	291 [1.435], 322 [1.175]	516	(0.22, 0.54)	1.2
$CHCl_3$	294 [1.367], 327 [1.321]	421, 510	(0.19, 0.48)	1.0
Dioxane	290 [1.000], 323 [0.910]	416, 507	(0.19, 0.46)	1.5
Acetone	329 [1.435]	512	(0.21, 0.55)	1.1
CH_3CN	291 [1.231], 324 [1.278]	507	(0.18, 0.40)	1.0
DMF	295 [1.038], 329 [1.251]	522	(0.22, 0.44)	1.0
CH_3OH	291 [1.592], 321 [1.291]	516	(0.22, 0.57)	1.1
DMSO	294 [0.969], 330 [1.125]	521	(0.24, 0.48)	1.1

Table S3. Molar absorption coefficients, emission spectral data, CIE chromaticity coordinates and quantum yields of metallacycle **3b** in different solvents (c = 10.0 μM, λ_{ex} = 365 nm).

Solvents	λ_{ab} / nm [$\varepsilon \times 10^5$, $cm^{-1}\ M^{-1}$]	λ_{em} / nm	CIE	Φ (%)
CH_2Cl_2	327 [2.375], 448 [0.346]	513, 571	(0.43, 0.51)	3.6
THF	328 [1.906], 472 [0.384]	511, 576	(0.47, 0.50)	3.3
EA	330 [0.484]	508	(0.20, 0.58)	7.0
C_2H_5OH	325 [1.552], 462 [0.265]	531, 575	(0.46, 0.52)	2.8
$CHCl_3$	327 [1.967], 454 [0.314]	506, 578	(0.46, 0.49)	2.5
Dioxane	327 [1.742], 448 [0.257]	512, 556	(0.31, 0.57)	6.9
Acetone	334 [1.938], 457 [0.363]	511, 572	(0.45, 0.52)	3.6
CH_3CN	311[1.713], 322 [1.703], 428 [0.243]	519	(0.26, 0.62)	11.2
DMF	327 [1.700], 459 [0.314]	535	(0.34, 0.61)	6.2
CH_3OH	325 [2.203], 457 [0.379]	580	(0.51, 0.48)	2.4
DMSO	325 [1.793], 455 [0.343]	544	(0.38, 0.59)	4.4

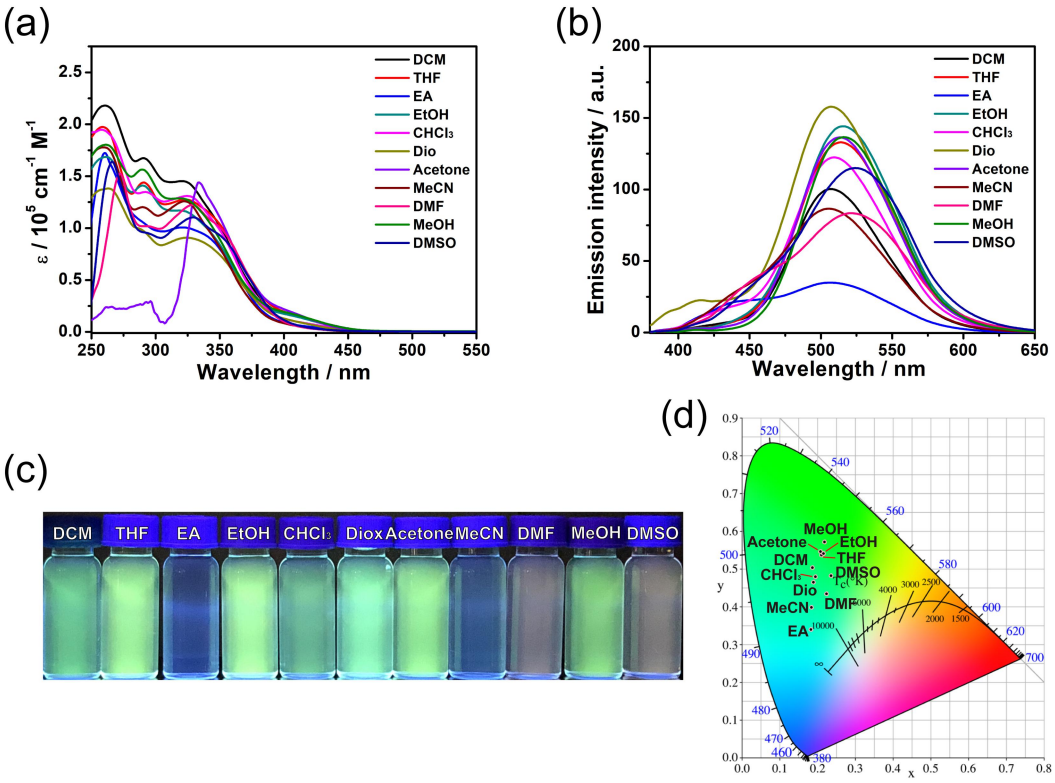

Figure S44. (a) Absorption and (b) emission spectral profiles of metallacycle **3c** in different solvents; (c) Images of metallacycle **3c** under UV lamp in different solvents. (d) CIE chromaticity coordinates of metallacycle **3c** in different solvents (c = 10.0 μM, λ_{ex} = 365 nm).

Table S4. Molar absorption coefficients, emission spectral data, CIE chromaticity coordinates and quantum yields of metallacycle **3c** in different solvents (c = 10.0 μM, λ_{ex} = 365 nm).

Solvents	λ_{ab} / nm [$\varepsilon \times 10^5$, $cm^{-1}\ M^{-1}$]	λ_{em} / nm	CIE	Φ (%)
CH_2Cl_2	326 [2.589], 443 [0.42]	453, 541	(0.27, 0.46)	5.8
THF	324 [2.489], 440 [0.461]	467, 541	(0.20, 0.33)	5.3
EA	303 [0.521]	457	(0.14, 0.11)	8.1
C_2H_5OH	322 [1.81], 433 [0.327]	478, 537	(0.25, 0.48)	5.4
$CHCl_3$	326 [2.346], 442 [0.405]	453, 547	(0.31, 0.51)	5.2
Dioxane	312 [1.709], 435 [0.225]	460	(0.15, 0.16)	10.5
Acetone	332 [2.066], 433 [0.437]	469, 539	(0.19, 0.31)	4.0
CH_3CN	302 [1.501], 324 [1.272], 402 [0.281]	463	(0.14, 0.14)	22.8
DMF	326 [1.478], 416 [0.293]	476	(0.15, 0.28)	11.0
CH_3OH	314 [2.799], 432 [0.521]	541	(0.34, 0.61)	2.6
DMSO	324 [1.995], 432 [0.366]	488	(0.18,0.39)	9.4

*5. Optical characterization data of metallacycle **3a** and **3c** in $CHCl_3$/hexane*

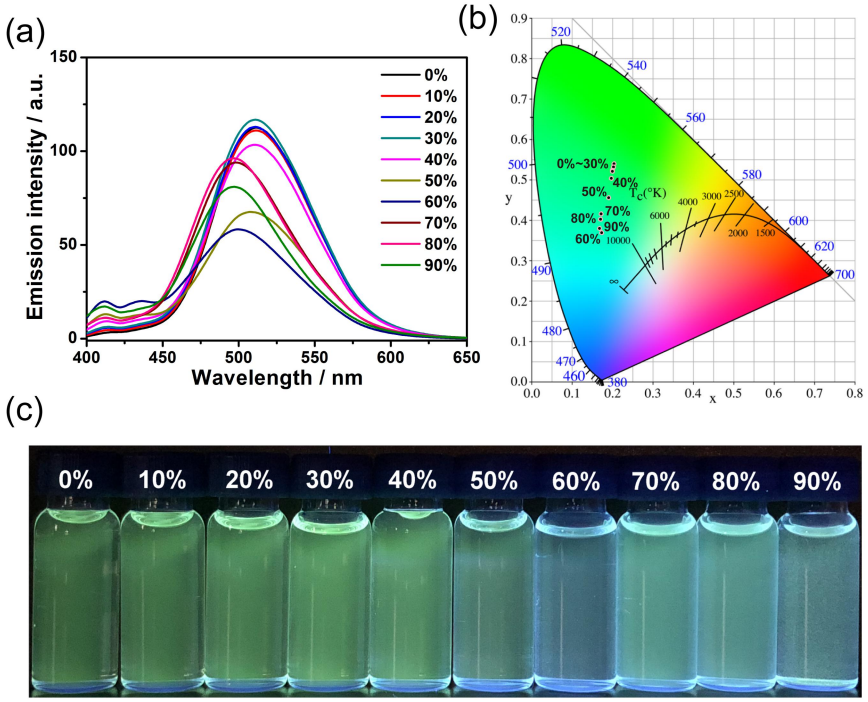

Figure S45. (a) Emission spectral profiles and (b) CIE chromaticity coordinates of metallacycle **3a** in $CHCl_3$/hexane mixture under conditions of varying hexane content. (c) Images of metallacycle **3a** under UV lamp in $CHCl_3$/hexane mixture (c = 10.0 μM, λ_{ex} = 365 nm).

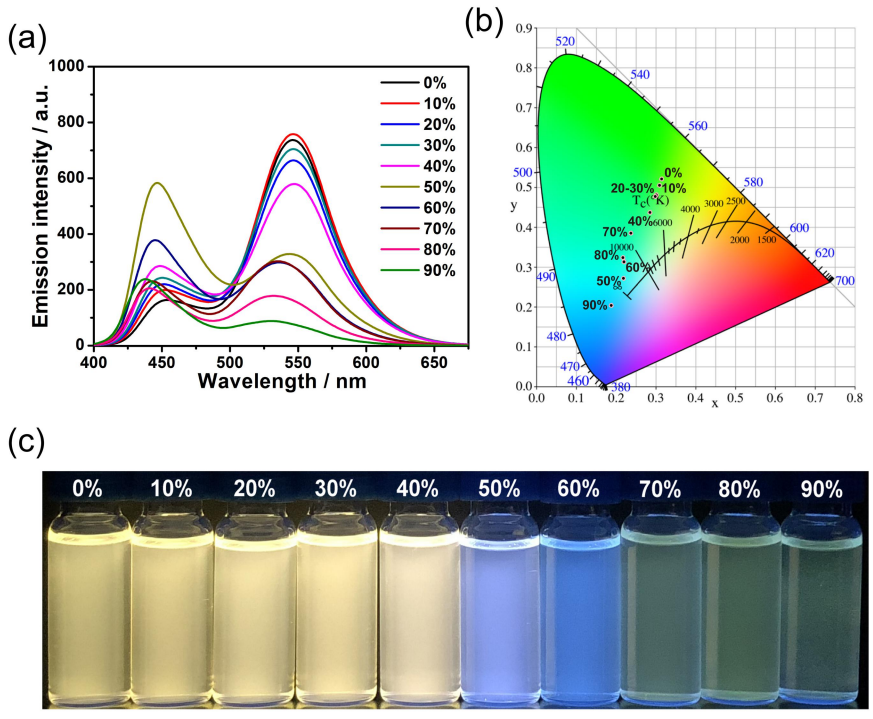

Figure S46. (a) Emission spectral profiles and (b) CIE chromaticity coordinates of metallacycle **3c** in $CHCl_3$/hexane mixture under conditions of varying hexane content. (c) Images of metallacycle **3c** under UV lamp in $CHCl_3$/hexane mixture (c = 10.0 μM, λ_{ex} = 365 nm).

*6. Morphology of micelles based on metallacycle **3a** and **3c***

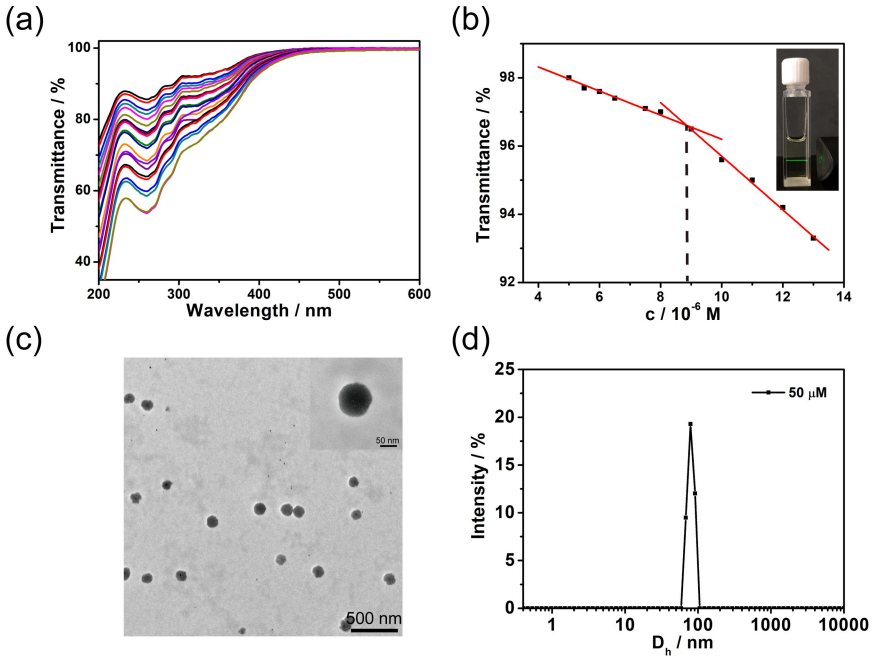

Figure S47. (a) UV–vis absorption spectral profiles of metallacycle **3a** at different concentrations. (b) Concentration-dependent optical transmittance and Tyndall effect observed for metallacycle **3a**. (c) TEM images of metallacycle **3a** (scale bar is 500 nm and 50 nm). (d) Size distribution of metallacycle **3a** in the CH_3OH/H_2O (6/94, *v*/*v*) solvent system.

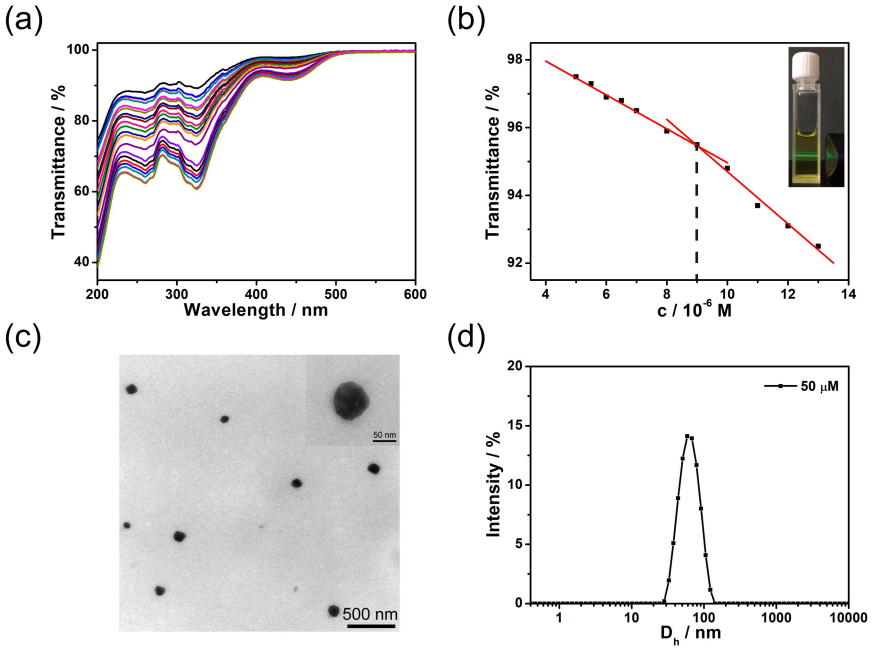

Figure S48. (a) UV–vis absorption spectral profiles of metallacycle **3c** at different concentrations. (b) Concentration-dependent optical transmittance and Tyndall effect observed for metallacycle **3c**. (c) TEM images of metallacycle **3c** (scale bar is 500 nm and 50 nm). (d) Size distribution of metallacycle **3c** in the CH_3OH/H_2O (6/94, *v*/*v*) solvent system.

7. Cell imaging

The CT26 and RAW264.7 cell lines were purchased from American Type Culture Collection (ATCC, Rockville, MD). The CT26 and RAW264.7 cells were cultured in Dulbecco's modified eagle medium (DMEM) containing 10% fetal bovine serum (FBS) and grown under humidified air containing 5% CO_2 at 37 °C.

The cytotoxicity of Pt(II) acceptor, ligands **1** and metallacycles **3** were evaluated by MTT assay using CT26 and RAW264.7 cells. Generally, the cells were seeded on a 96-well plate at a density of 1×10^4 cells/well in 200 μL of DMEM medium containing 10% serum for 18 h separately. The culture medium was replaced by serum-free medium containing serial various concentrations of Pt(II) acceptor, ligands **1** and metallacycles **3** for 24 h. The MTT solution was added to the wells to achieve a final concentration of 0.5 mg mL^{-1}. After incubation for another 24 h, each well was replaced with 100 μL of DMSO and measured spectrophotometrically on an ELISA plate reader (Model 550, Bio-Rad) at a wavelength of 570 nm. The relative cell growth (%) related to control cells cultured in the medium without the polymer was calculated by the following formula: $V\% = ([A]_{experimental} - [A]_{blank}) / ([A]_{control} - [A]_{blank}) \times 100\%$. Where $V\%$ is the relative cell viability (%), $[A]_{experimental}$ is the absorbance of the wells culturing the treated cells, $[A]_{blank}$ is the absorbance of the blank, and $[A]_{control}$ is the absorbance of the wells culturing untreated cells.

The cell uptake was examined by laser scanning confocal microscopy. CT26 cells were seeded onto 12-well plates and grown for 18 h, then treated with ligands **1** and metallacycles **3** at the concentration of 20 μg mL^{-1} per well. The medium was removed after incubation 4 h, then the cells were washed twice with PBS and fixed with 4% formaldehyde for 10 min and treated with 200 μL DiO for 30 min. The confocal images were acquired on a confocal scanning laser microscope (CLSM, Radiance 2100, Bio-Rad). Flow cytometry was used to quantitatively evaluate the cellular uptake. 2×10^5 Cells/well of CT26 cells were seeded in 6-well plates and cultured at 37 °C for 18 h. Ligands **1** and metallacycles **3** solutions were added to each well (20 μg mL^{-1}). Ligands **1** and metallacycles **3**-free culture medium was applied as a blank control. After 4 h incubation at 37 ℃, cells were rinsed with PBS, harvested by trypsinization (without EDTA), centrifuged (1000 rpm, 10 min), and resuspended in PBS. The fluorescence intensities of ligands **1** and metallacycles **3** were measured by a FACS Calibur flow cytometer (BD Biosciences, USA).

8. References

[S1] B. Sun, S. S. Nurttila, J. N. H. Reek, Synthesis and characterization of self-assembled chiral $Fe^{II}_2L_3$ cages, *Chem. Eur. J.* **2018**, *24*, 14693–14700.

[S2] M. Zhang, S. Yin, J. Zhang, Z. Zhou, M. L. Saha, C. Lu, P. J. Stang, Metallacycle-cored supramolecular assemblies with tunable fluorescence including white-light emission, *Proc. Natl. Acad. Sci. USA* **2017**, *114*, 3044–3049.

[S3] R. Sato, J. Kozuka, M. Ueda, R. Mishima, Y. Kumagai, A. Yoshimura, M. Minoshima, S. Mizukami, K. Kikuchi, Intracellular protein-labeling probes for multicolor single-molecule imaging of immune receptor-adaptor molecular dynamics, *J. Am. Chem. Soc.* **2017**, *139*, 17397–17404.